ADVANCED OPTICAL MATERIALS
www.advopticalmat.de

Fiber Optic Devices for Diagnostics and Therapy in Photomedicine

Yubing Hu, Paolo Minzioni, Jie Hui, Seok-Hyun Yun, and Ali K. Yetisen**

Photonic technologies have made enormous impacts on modern medicine, advancing disease diagnostics and treatments as well as health monitoring. A long-standing challenge in the use of light and its widespread effects in photomedicine is the finite penetration of light in tissues. However, judiciously engineered optical fibers helped overcome this challenge and advance light delivery to deep tissues with spatial precision and desired accessibility. In recent years, the development of photonic technologies including optical biomaterials, fiber functionalization, and biomedical device innovations has greatly expanded the scope of light-based healthcare. Here, the fundamentals and materials of fiber optics to endow themselves with biocompatibility, flexibility, and diverse functionalities required for long-term implantation are overviewed. The design strategies of lab-on-fiber techniques, operation requirements to construct fiber optic sensors, and their health monitoring applications as wearable and implantable devices are presented. The use of fiber optics in major light-based therapeutic modalities including optogenetics, photodynamic therapy, photobiomodulation, photochemical cross–linking, and photothermal therapy is illustrated to enhance their effectiveness, specificity, and feasibility. In short, a comprehensive review is provided on the fiber optic techniques and the latest photonic devices, which are envisioned to evolve photomedicine in clinical and point-of-care practices.

1. Introduction

Photomedicine is a multidisciplinary field encompassing the utilities of light and its effects on improving health and advancing biomedical sciences. Extensive phototherapy studies have been carried out during the last 30 years, advancing the light-based opportunities for treating cancer,[1] skin diseases,[2] and infections.[3] Historically, Niels Finsen received the Nobel Prize in Physiology and Medicine in 1903 for demonstrating the treatment of *lupus vulgaris* with light.[4] Blue light therapy has been widely utilized as the gold standard to treat newborn jaundice since 1968, which diminishes the high bilirubin level and prevents its neurotoxic effects.[5] The first research lab dedicated to this field, which now has become the Wellman Center for Photomedicine, was established in 1975 after the discovery of a photoactive drug to treat psoriasis[6] and pioneered numerous dermatologic and cosmetic applications of lasers. At the state of the art, light can be used not only as a therapeutic drug but also as a precise sensor, a diagnostic tool, and a localized therapy activator. The remarkable examples of photomedicine applications in current clinical practice range from infrared thermometers, X-rays, computed tomography (CT),[7] endoscopy,[8] optical coherence tomography (OCT),[9] laser-assisted in situ keratomileusis (LASIK) eye surgery to photodynamic therapy (PDT).[10] These light applications in medical diagnosis and therapy are rooted in the light absorption and scattering of the intrinsic biomaterials or exogenous light-active regents.[11] One of the most fundamental challenges in using light for medical applications originates from the finite optical penetration depth of light, typically no more than a few millimeters in tissue.[12] This limitation highlights the need for effective and low-cost light-delivering methods, for which optical fibers emerge as practical solutions.[13] Optical fibers have attracted considerable attention for their light-guiding efficiency, spatial precision, deep tissue penetration, minimal invasiveness, easy miniaturization, and cost-effectiveness. Benefiting from these advantages, fiber optic devices have proved to be a powerful platform for various diagnostic and/or therapeutic applications.[14]

Optical fibers have been employed as optical waveguides in medical devices since the 1960s when bundled fibers were pioneered for imaging through catheter-based endoscopes.[15] In the late 1980s, fiber optic imaging-guided techniques were accepted

Y. Hu, A. K. Yetisen
Department of Chemical Engineering
Imperial College London
London SW7 2AZ, UK
E-mail: a.yetisen@imperial.ac.uk
P. Minzioni
Department of Electrical
Computer and Biomedical Engineering
University of Pavia
Pavia 27100, Italy
J. Hui, S.-H. Yun
Harvard Medical School and Wellman Center for Photomedicine
Massachusetts General Hospital
Boston, MA 02114, USA
E-mail: syun@mgh.harvard.edu
J. Hui, S.-H. Yun
Harvard–MIT Health Sciences and Technology
Cambridge, MA 02139, USA
The ORCID identification number(s) for the author(s) of this article can be found under https://doi.org/10.1002/adom.202400478

DOI: 10.1002/adom.202400478

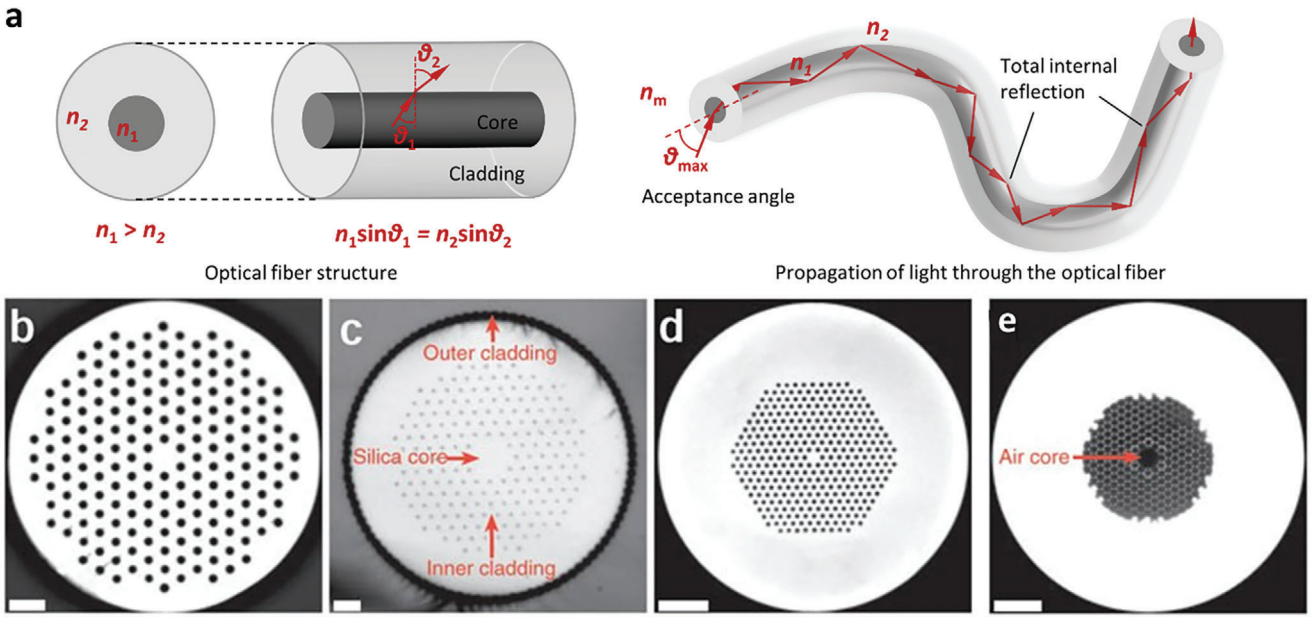

Figure 1. Structure of optical fibers. a) Schematical representation of an optical fiber. The cross–section (left) is composed of two concentric discs, the inner one corresponds to the fiber core, and the external one to the fiber cladding. The longitudinal Section (right) allows for showing the angles involved in Snell's law. b–e) Cross–sections of different photonic crystal fibers. b–d) The core is constituted by a solid-glass region and the guiding effect can be obtained both by an effective-index effect (i.e., the "effective index" in the cladding region is lower than that of the core because of the presence of air holes) or thanks to the creation of a photonic crystal structure. e) The fiber core is constituted by a hollow region of the fiber (i.e., generally filled with air), and the guiding effect is obtained thanks to a precise design of lateral holes (geometry, size, position), creating a highly reflective region for the light propagating in the core. Adapted with permission from.[23]

for minimally invasive surgery like laparoscopic surgery.[16] More recently, the fabrication of nonconventional optical fibers with high elasticity, biocompatibility, easy functionalization, and even biodegradability has been demonstrated.[17] The availability of low-cost, miniature fiber optic biosensors is particularly beneficial for point-of-care and intensive-care diagnostics.[18] Minimal invasive, patient-compliant optical fibers are emerging for various fiber-optic therapeutic strategies.[19] The global market for fiber optics in the sector of biophotonics is large and expanding, which was estimated to be 880 million dollars in 2020 and is expected to reach 1.5 billion dollars by 2030.[20] It is fueled predominantly by the increasing preference for minimally invasive surgery procedures, the advancement in new medical devices, the growing use of lasers in dentistry, and the rapid development of new biomedical fiber sensors.[21] The current market of phototherapy devices is at a level of 800 million dollars with a compound annual growth rate of 4.75%.[22] The prospective rapid growth in photomedicine states the urgent need for technological innovations in fiber optic instruments and practical applications in biomedical diagnostics and therapies.

Recent advances in materials and light-derived technologies are accelerating the implementation of fiber optic devices for advanced diagnostics and therapies. Fiber optic devices are becoming increasingly ubiquitous owing to the continuing development of fiber materials, fabrication techniques, sensing functionalization, diagnostic platforms, therapeutic modalities, and clinical applications. Over the past decades, these technological advances have particularly reduced the cost by making light-based diagnostics and therapies more accessible. Here, we describe the basic optical fiber structure and different materials in Section 2, which will facilitate the selection of optical fibers for the desired medical applications. In Section 3, the fiber optic sensing devices are overviewed, including their commonly used design principles and their diagnostic applications as wearable and implantable devices. In Section 4, we introduce the working principles of major phototherapy modalities and showcase their latest fiber optic innovations. Furthermore, the unmet challenges and prospects are discussed to predict the next-generation advances in fiber optic diagnostics and therapies, illuminating the bright future of biomedical photonics in clinical and point-of-care settings.

2. Optical Fiber Materials

2.1. General Description

The simplest structure of an optical fiber is composed of two coaxial cylinders realized using two slightly different materials as shown in **Figure 1a**. The external cylinder is called the "cladding" (of refractive index n_2), while the internal one is identified as the "core" (having a refractive index $n_1 > n_2$), and beam confinement occurs thanks to the principle of total internal reflection. In a minority of cases, optical waveguiding can also be obtained using a different approach, where the core and cladding regions are not simply defined by the refractive indices of the constituent materials, but by the more sophisticated geometry of the regions, generally constituted by a multi-layer or holy structure with specific geometrical parameters. Several exemplary structures are shown in Figure 1b–e. Those kinds of structures can exhibit peculiar properties, allowing for example the realization of "hollow core" fibers (Figure 1e).[23]

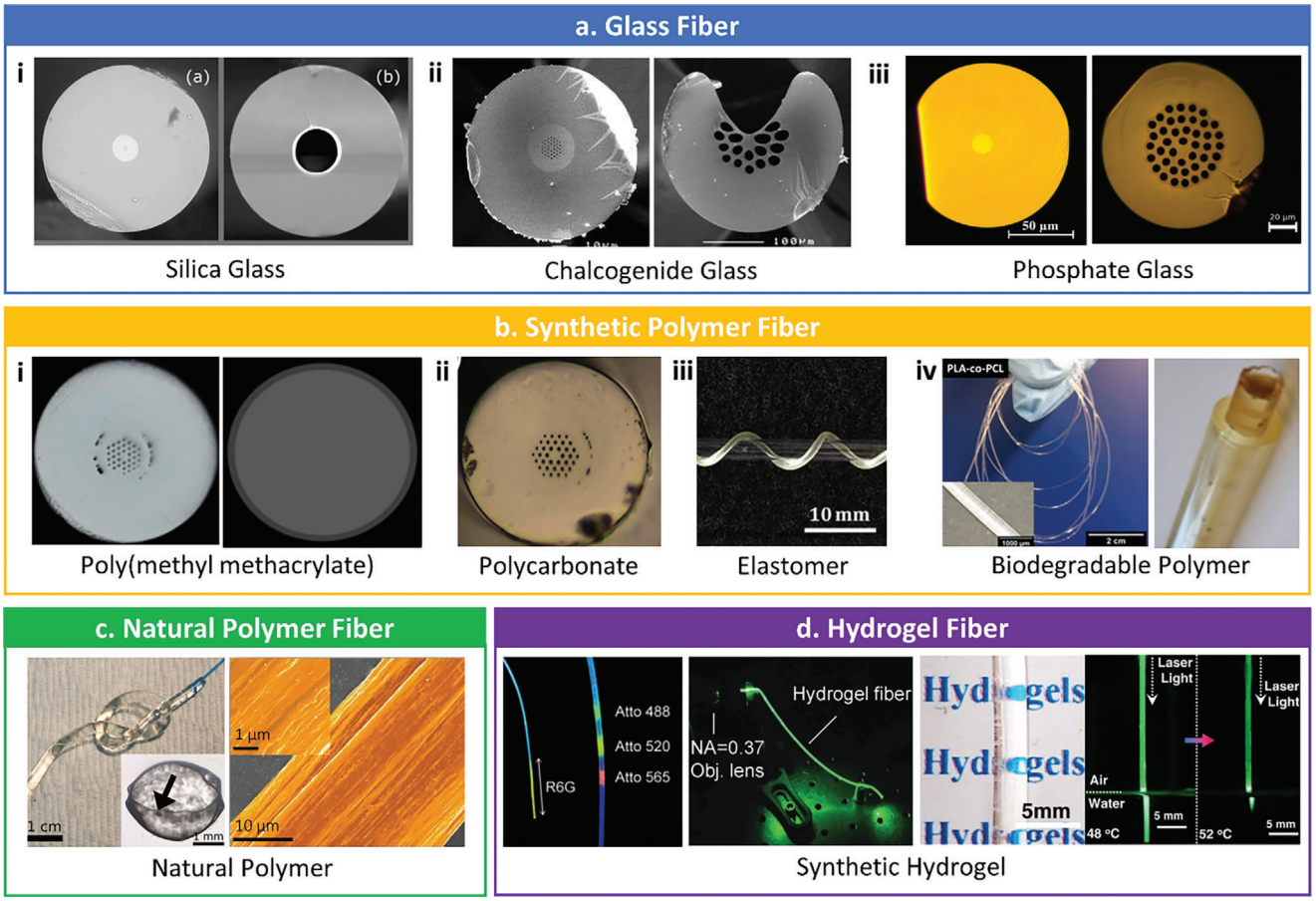

Figure 2. Fiber materials. a) Glass fibers: i) silica glass fibers adapted from ref. [24] ii) chalcogenide glasses adapted from ref. [25,26] iii) phosphate glasses adapted from ref. [27,28] b) Synthetic polymer fibers: PMMA adapted from ref. [29] ii) polycarbonate adapted from ref. [30] iii) elastomers adapted from ref. [31] iv) biodegradable synthetic polymers adapted from ref. [32,33] c) Natural polymer fibers adapted from ref. [34,35] d) Hydrogel fibers: synthetic hydrogels adapted from ref. [36–38].

Fibers are commonly differentiated into single-mode and multimode based on their ability to guide light signals and the mode of propagation within the fiber. Single-mode fibers have a small core diameter (typically ≈8–10 µm) which allows only one mode of light propagation, enabling the transmission of light with minimal dispersion. Single-mode fibers are optimized for applications requiring precise signal transmission or long distances with low signal loss, such as endoscopy and optical coherence tomography for high-resolution imaging. Multimode fibers have a larger core diameter (typically between 50–100 µm), offering easier coupling of light sources, having transmission capability of higher optical power, and allowing multiple modes of light to propagate simultaneously. Multimode fibers are suitable for applications where higher light intensity or larger beam diameter is needed over shorter distances, including photodynamic therapy and laser surgery. Moreover, multimode fibers can facilitate multiplexed signal detection or parallel analysis of multiple samples, leading to faster data acquisition and higher throughput in sensing applications.

In the following, we discuss the most used materials including the backbone materials for the core and cladding and functional dopants added to the backbone materials to change refractive index or incorporate desired optical properties. As optical fiber properties depend on a large set of parameters (materials, size, fabrication procedure, surface treatments, etc.), this work intends to offer only a major reference frame. As shown in **Figure 2**, we divide the materials used for the realization of optical fibers into four principal categories according to the used backbone material: 1) glasses; 2) synthetic polymers; 3) natural polymers; and 4) hydrogels.

2.2. Glasses

Glasses are a fundamental class of fiber optic materials (Figure 2a). Glasses offer excellent transparency and low optical losses, making them ideal for long-distance optical communication and high-power laser transmission. Their chemical stability and mechanical strength ensure reliability in various harsh environments. The traditional optical fibers are generally obtained using fused silica (SiO_2) both as a core and cladding material. SiO_2-based fiber generally shows very low propagation losses, but high Young's modulus, which corresponds to a material significantly more rigid than biological tissues. The most used

silica fiber, the Corning SMF-28, has a core radius of 4.1 μm, and scattering-limited propagation loss of 0.2 dB km^{-1} for a wavelength ≈1550 nm. In the visible wavelength range (generally more interesting for biomedical applications), the attenuation of silica fibers is ≈3–5 dB km^{-1} for red light, 30–50 dB km^{-1} for green light, and almost 100 dB km^{-1} for blue light. Although silica is a biocompatible material, the implantation of common silicate glasses in a tissue will generally produce a thick non-adherent capsule due to the foreign body reaction. Additionally, the low mechanical resistance of glass fibers, if not properly protected with additional layers, may cause fiber breaking, and the high axial rigidity with respect to normal tissues may cause localized damage.

Special attention, in this category, must be paid to optical fibers based on bioresorbable glass. Phosphate glasses are a particularly good candidate as their degradation time in aqueous media can be precisely controlled by modifying glass composition.[39] Their biological compatibility has been investigated[40] and the possibility to obtain nontoxic, resorbable glasses, suitable for fiber drawing was demonstrated.[27] Optical fibers with a 120 μm outer diameter and a 12 μm core diameter were demonstrated by the standard drawing approach and exhibited propagation losses lower than 0.02 dB cm^{-1} at 1300 nm and lower than 0.05 dB cm^{-1} at 633 nm, thus allowing easy transport of the radiation within a distance suitable for biomedical applications. The wide transparency window of these materials, ranging from UV (240 nm) to NIR (2500 nm), allows using standard techniques, such as phase-mask UV writing technique, to realize optical sensors directly embedded within the fiber.[41] A review dedicated to the fabrication and characterization of phosphate glasses with good optical quality and high resorbability can be found elsewhere.[42]

2.3. Synthetic Polymers

Synthetic polymers, including plastics, elastomers, and biodegradable polymers, play a crucial role in fiber optics due to their flexibility, low cost, and ease of processing (Figure 2b). Plastic optical fibers (POFs)[29] were initially developed almost at the same time as silica fibers, but their high attenuation, low-temperature tolerance, and the lack of well-established fabrication technologies didn't make them competitive for long-distance transmission. Multimode POFs cores are generally made of poly(methyl methacrylate) (PMMA), whose refractive index (n_{PMMA} ≈ 1.49) is slightly higher than silica glass (n_{SiO2} ≈ 1.45) and have a typical core radius generally in the range 20–100 μm, supporting the propagation of 10^3–10^5 optical modes. PMMA fibers, after proper cladding decoration (see Section 3.1) have already been demonstrated as a suitable medium to realize photobiomodulation devices (see Section 4.3). Single-mode POFs, whose performances are gradually improving over time at low cost,[43] are used for high-precision sensors.[44] With respect to their silica equivalent, the POF-based sensors have the inherent advantages of lower cost, higher fracture resistance, and higher biocompatibility.

Elastomers, characterized by extreme flexibility and large deformability, are particularly well suited for the realization of optical sensors requiring to be inserted in fabrics, as required for the development of wearable optical sensors (see Section 3.2). In optical applications, the most used elastomer is polydimethylsiloxane (PDMS), which is well-known in the electronic industry for its elasticity, chemical inertness, and thermal stability. PDMS can be easily shaped into different shapes, it shows a wide transparency window, and its refractive index (n = 1.42) is sufficiently high to allow optical guiding with attenuation values as low as 0.5 dB cm^{-1} in the visible range. Recently a biodegradable elastomer fiber based on poly-octamethylene-maleate-citrate core and a poly-octamethylene-citrate cladding has been demonstrated with a relatively low loss of 0.4 dB cm^{-1}.[31] This is obtained owing to the use of citrate-based elastomers, whose degradation time can be modified by changing the synthesis process.

Biodegradable polymers offer advantages in terms of biocompatibility and degradation properties, making them suitable for implantable medical devices and tissue engineering scaffolds. These materials enable minimally invasive optical sensing and imaging within biological systems without causing adverse reactions. The most commonly investigated biodegradable materials are based on poly(ethylene glycol) (PEG), poly(lactic acid) (PLA), poly(glycolic-acid) (PGA), and poly(caprolactone) (PCL), as well as their copolymers and derivatives. By controlling the polymer preparation conditions, and the presence of copolymers, it is possible to fine-tune the final mechanical, optical, and chemical properties. In general, synthetic polymers show a relatively high refractive index (>1.45),[32] low optical attenuation, and tunable mechanical flexibility. For example, optical fibers cut from PLA flexible films have shown a propagation loss of 1.5 dB cm^{-1} in air and 6.2 dB cm^{-1} in water.[12] Lower losses were obtained by using a 3D extrusion printer and by proper nozzle selection.[32] Fibers of pure PLA (core-only) showed a relatively low attenuation of 0.08 dB cm^{-1} in air, and lower than 0.3 dB cm^{-1} when inserted into porcine tissue. Extensive literature is also available regarding the biocompatibility and biodegradability of these polymers.[45] When inserted in a live organism, these polymers can be slowly degraded by natural processes such as hydrolysis and zymolysis, leaving only non-toxic molecules (or low-toxicity compounds) because of the process, which can then be absorbed or excreted by the body naturally, thus not requiring any surgery to remove the implant after usage. Biodegradable, and soft PLLA fibers were demonstrated for in-vivo neural signal sensing and interrogation in mice. In that case, core-only fibers showed an attenuation of 0.9 dB cm^{-1} when embedded in brain tissues.[46]

2.4. Natural Polymers

Nature offers great inspiration in the biomedical field for the design of engineering solutions. Large attention has been paid to the optimization of optical materials inspired or derived by natural polymers. The use of natural materials could produce optical fibers without using fossil resources, potentially opening the way for a "green photonics" development (Figure 2c). Optical fibers based on cellulose were successfully demonstrated >15 years ago,[47] but due to the delicate structure of the fibers and to the lack of optimized fabrication protocols the optical attenuation showed by cellulose-based materials is still high (≈6 dB cm^{-1}).[48] Silk represents an interesting natural polymer for optical fibers. The most widely investigated silk material is obtained by processing the *Bombyx mori* (a worm) silk filament. The silk fibroin

solution obtained after proper processing can be used for the creation of different optical components, including gratings,[49] mirrors,[50] inverse opals,[51] or optical fibers.[34] A silk optical fiber using fibroin as the core material ($n \approx 1.54$) and a silk hydrogel ($n \approx 1.34$) as a cladding material was realized by injection molding, and an attenuation of ≈ 2 dB cm^{-1} was measured.[34] Using recombinant engineering, silk with unusually high refractive index of ≈1.7 has been developed to demonstrate effective light guiding even without a cladding layer.

2.5. Hydrogels

Hydrogels are a large class of material, characterized by a very low Young's modulus and composed by a hydrophilic-polymer 3D network containing free water molecules. There has been considerable interest in making optical fibers out of hydrogel materials so that they have similar physical and mechanical properties as tissues (Figure 2d). One of the unique features of hydrogels is that their properties are critically dependent on their water content. Owing to their favorable mechanical properties, and their large water content, hydrogels have been demonstrated as suitable candidates for the realization of implantable devices with programmable degradation rates.[52] The most commonly used hydrogels are based on 3D-networks of PEG ($n \approx 1.46$) and its derivatives as PEG-diacrylate (PEGDA) and copolymers of PEGDA and polyacrylamide (PAAM). Hydrogels can be used for both cores and clads or only for cladding in conjunction with higher refractive index core materials.[53] When considering the realization of hydrogel fibers, particular attention is required to the mechanical properties of the material as conventional hydrogels tend to have lower mechanical strength and may break under high external stress. For this reason, the development of highly stretchable hydrogels, suitable to be used also for in-vivo application, is of the utmost importance.[37] At the state of the art, both sensors (oxygenation, glucose) and light delivery systems for phototherapy applications have been demonstrated using hydrogels.[36]

2.6. Mechanical Properties and Optical Loss

The mechanical and optical properties of various material options in **Figure 3** are to be properly considered when designing a fiber-based light delivery system for specific applications. In general, when designing implantable devices, it is important to use materials with appropriate Young's modulus values, so as to match the mechanical properties of the surrounding tissues, in order to limit the risks of implant breakage, implant displacement, or tissue damage. As a reference, biological tissues have Young's modulus in the range between 1 to 100 kPa for soft tissues while it is ≈1 MPa for tendons and 100 GPa for bones. Considering the implant of a general device (not exclusively a fiber) in a soft tissue such as a muscle, different problems may arise in case the device Young's modulus is not properly selected. If the Young's modulus of the implant material is too high, the implant may cause excessive stress on the surrounding tissue, leading to tissue damage, and inflammation, and consequently producing discomfort or pain to the patient and implant failure. If Young's modulus of the implant material is too low, the implant may not be able to provide enough stability, leading to implant displacement or migration, which can cause discomfort, pain, or even yield internal injuries to the patient.

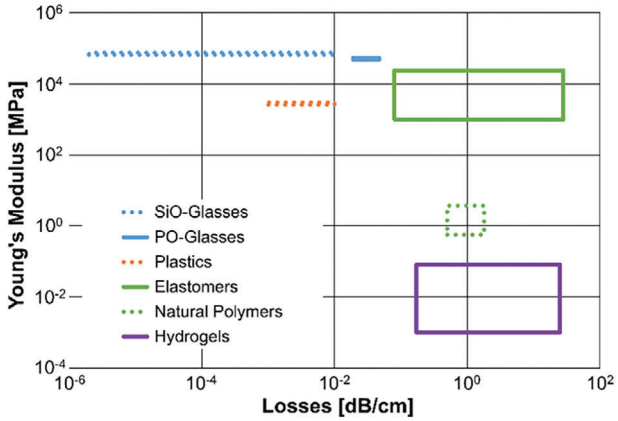

Figure 3. Propagation loss and Young's modulus of different optical materials used for optical waveguiding. The data was extracted from ref. [17,54–56] Bioresorbable materials are indicated by a continuous line, while non-bioresorbable ones with a dotted line.

Optical loss is a key property as it determines how much light will reach the fiber end and how much will be scattered along the fiber, potentially yielding undesired effects in surrounding tissues. Finding the ideal tradeoff between low Young's modulus and low attenuation is not trivial because softer materials generally have higher losses compared to stiffer materials due to typically the large scattering size of macromolecules. The correct identification of the suitable alternatives thus strongly depends on the specific application.

3. Fiber Optic Sensors and Health Monitoring

Optical sensors can response to the physicochemical and biological variations and transduce the changes of photophysical properties to readable signals.[57,58] So far, most optical sensors are activated by free-space illumination, resulting in an inevitable light loss, especially for long-distance transport in medical diagnostics with strong light absorption and scattering. Extensive endeavors have been devoted to the explorations of optical sensors at precise locations.[59] Optical fibers present an ideal technological platform for in vivo diagnostics by controlling light from a remote location. Alternatively, an optical fiber itself can serve as the sensor. Currently, fiber optic sensors[60–63] have attracted considerable attention for their unique intrinsic advantages including lightweight, long sensing length, remote detection, high sensitivity, high selectivity, immunity to electromagnetic interference, and so on. Herein, we summarize the fabrication and operation methods of fiber optic sensors and showcase their device innovations for medical diagnostics.

3.1. General Design of Fiber Optic Sensors

The development of materials and manufacture technology in fiber optics has evolved the conventional silica fibers with

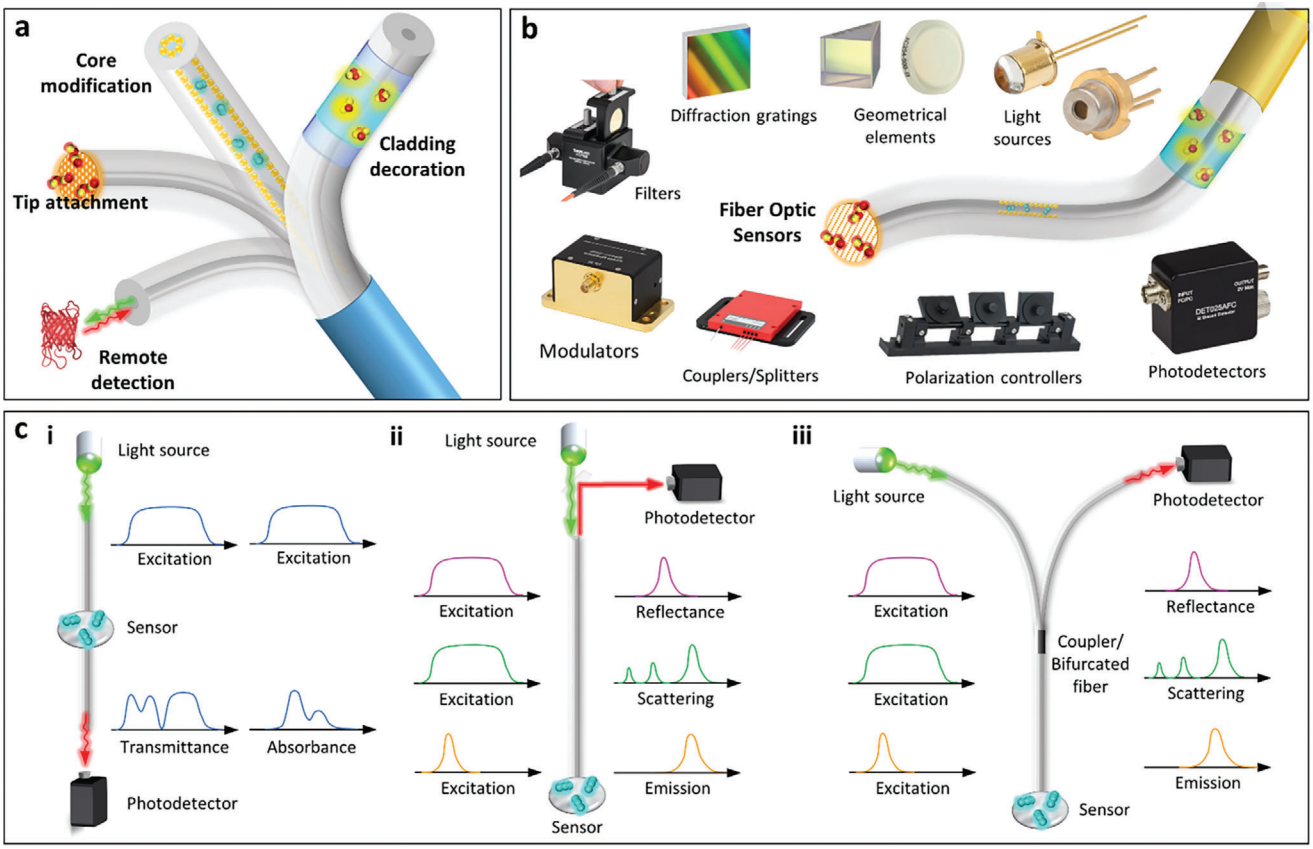

Figure 4. Construction of fiber optic sensor devices. a) Fabrication of fiber optic sensors by core modification, cladding decoration, tip attachment, and remote detection. b) Optical components to illuminate, regulate, collect, and analyze light for fiber optic sensors. For the operation of fiber optic sensors, it requires a light source to excite the fiber optic system with the optical sensors and a photodetector to measure the optical signals emitted from the sensing area. Adapted from Thorlabs, Inc 1999–2023. c) Working modes of optical fiber sensors including i) sensor-in-fiber in the individual fiber, ii) sensor-on-tip in the individual fiber with a semi-transparent mirror, iii) sensor-on-tip based on fiber coupler or bifurcated fiber. The sensing systems allow the detection of various changes in light transmission, absorbance, reflectance, scattering, and emission. The light-sensor-analyte interactions modify the light properties according to the characteristics of the analyte, and thus the changes of light are used to qualify or quantify the analyte.

uniformly doped core and simple cladding structures to the advanced multi-structural and multi-functional optical fibers.[64] The lab-on-fiber technology[65,66] to integrate the functionalities of fiber at micro- and nano-scales firmly supports the development of biochemical sensing and medical diagnosis. The following four categories are classified by the position of the light–matter interaction[18] (**Figure** 4a).

Cladding decoration refers to the functionality integrated into the outer cylindrical region of a core/cladding optical fiber, where the extraction of the evanescent field enables the light-matter interactions. According to the light extraction mechanism, this fiber configuration can be achieved through two main approaches: 1) evanescent field exposed by tapered/unclad/D-shaped/U-shaped fibers; 2) diffraction gratings into the cladding through the introduction of periodic RI modulation in the core. The evanescent field exposed sensors can be integrated with diverse working principles including RI variations, absorption, reflection, fluorescence, lossy mode resonance (LMR), surface plasmon resonance (SPR), and whispering gallery mode (WGM) resonance. Moreover, this technique can be employed for multiplexed detection at different locations because of its advantages of sensing over long distances and large areas. Its drawbacks include large device size, high insertion loss, and complex fabrication technologies.

Core modification refers to the functionality integrated within the core of the fiber, where the functional materials, microfluidics, and photonics are incorporated along the entire fiber length. Bragg-grating fibers have been proposed for shape sensing in surgical robotic arms. Since the 1980s, photonic crystal fibers (PCFs) have been widely studied to trap the light inside a hollow fiber with periodic lattice of microscopic air holes.[67,68] The in-fiber microfluidics mainly consist of hollow, solid, and heterogeneous cores with filling materials. The hollow core enables the surface functionality of the core and liquid filling for extensive sensor explorations. Meanwhile, selective access to the core or cladding microfluidics can be rationally designed to exploit the light-matter interactions by the promotion of the synergistic combination with photonics as optofluidics.[69] Optofluidics has emerged as a novel analytical technique owing to the large surface-to-volume ratio, high sensitivity, and built-in fluidic channels for rapid and high throughput analyte delivery.

Tip attachment refers to the micro or nanostructures and functionality integrated into the microscale tip of optical fiber, which provides the inherently light-coupled platform for light-matter

interactions. A variety of micro and nanotechnologies have been utilized for the detection at the fiber tip. For example, metal nanoparticles are deposited at the end facet for label-free sensing through localized surface plasmon resonance (LSPR) and surface-enhanced Raman scattering (SERS). The plasmonic and photonic nanostructures as periodic gratings are inscribed for the enhancement of the electromagnetic field. Fabry-Perot cavity formed from two parallel reflection surfaces at the fiber tip is capable of RI differentiation. This fiber configuration demonstrates its unique advantages in biochemical sensing, such as ease of use, deep tissue accessibility, pin-point confined accuracy, available miniaturization, and low insertion losses. Meanwhile, the limitations of the tiny sensing area and short light–matter interaction distance serve as a trade-off.

Remote detection refers to the combination of extrinsic sensors outside the fiber, where the light-matter interactions occur remotely through free space coupling. Changes in extrinsic sensors arising from remote locations are very versatile since they can be detected alone, amplified, or detected in conjunction with wide-ranging optical methods. The simple and flexible combination with optical sensors makes this configuration easily accessible and multiplexed. The optical noise can be added during the external light path between the fiber and extrinsic sensors, which raises the requirements for the amplification of response signals. A typical example of remote detection is fiber photometry, in which the optical signals emitted from fluorescent sensors in the brain tissue are measured based on time-correlated single-photon counting fiber optics.[70]

Major optical components for the operation of fiber optic sensors are summarized in Figure 4b. Broadband sources such as the mercury vapor and halogen lamps are commonly used. Despite its high cost and sensitivity to temperature, the selective wavelength and high intensity of the laser make it a convenient and powerful excitation source. Light-emitting diodes (LEDs) have emerged due to their selective wavelengths, low cost, and long lifetime, while LEDs are slower and less efficient than lasers. Since the edge-emitting light sources emit light diverged at a large angle, it is desirable to use a fiber pigtail connection or microlens for focusing light. Photodetectors such as photodiodes, photomultiplier tubes (PMTs), and avalanche photodiodes (APDs) are commonly used for detecting and diagnosing light. Conventional benchtop spectrometers have been miniaturized into scaled-down spectrometer systems for portable and integrated applications recently.[71] The optical signal can be spectrally separated by a dichroic mirror, passed through a filter for removing excessive band pass, and then focused onto a photodetector.

The connection between the light source, sensing area, and photodetector in the fiber optic system is variable,[72] as depicted in Figure 4c. In general, excitation pulses are delivered to interact with the analyte, where the interaction changes the light properties in direction, intensity, wavelength, and polarization, and the modified light signals from the sensing area are measured by the photodetector. The light perturbation and noise caused by several factors need to be diminished for accurate sensing, including light source intensity fluctuation, optical fiber couplings between light sources, changes in fiber loss and attenuation, etc. The remote, variable, and robust operations of fiber optic devices make the fiber optic sensors remarkably attractive for biomedical applications ranging from point-of-care healthcare monitoring to clinical benchtop instrumentation. For example, a commercial, portable, and automated fiber optic biosensor system, RAPTOR has been invented for the simultaneous detection of four biological threats.[73] The RAPTOR system integrates all optics, electronics, fluidics, and software subsystems in a compact device. Based on the evanescent sensing, the RAPTOR performs rapid (5–13 min) and multistep sandwich fluorescent immunoassays on the surface of 4 polystyrene optical probes. Its successor the BioHawk has evolved as an 8-channel bioassay system with evanescent-wave interrogation on each waveguide.[74]

3.2. Wearable Sensing

Wearable sensors have attracted extensive interest for their potential to offer continuous, real-time, and noninvasive monitoring in biofluids via accessible sensor platforms (wristband, textile, mouthguard, contact lens, and microneedle patch).[75] Optical fibers can manipulate the delivery and expansion of light to the targeted sites with a minimum loss, which provides a reliable and efficient platform to integrate diverse sensory functionalities.

To mimic the simultaneous human visual and somatosensory responses of mechanical stimuli, the bimodal interactive fiber optoelectronics has been constructed.[76] Through the mechanical-induced optical and electrical changes via mechanoluminescent and triboelectricity, the self-powered optoelectronic fiber sensors (SOEFSs) can detect the mechanical stimulus quantitatively. The industrial-scale fabrication and recycling process of SOEFSs is achieved by modified Fermat spinning and melt-spinning. The helix structure of SOEFS enables a stable triboelectric signal under long-distance (≈80 m) and long-term (10 days) transmission. A highly stretchable and wearable textile using cotton as the weft and applying alternating the SOEFS and spandex as the warp was weaved (**Figure 5**a.i). When the smart textile was stretched in a warp direction, the luminescent signal was generated for direct observation, and the electrical signal was wirelessly transduced to the mobile phone. Furthermore, a cotton glove was integrated with the SOEFSs knitted in each finger, charge amplifier, battery, MCU, and wireless data transmitter (Figure 5a.ii). The separate finger motion sensing with quantitative analysis of finger bending angles and qualitative identification of stress was achieved, which inspires the exploration of multimode fiber optical sensors as smart textiles[77] for monitoring human motions and physiological signals.[78]

Moreover, fiber optic sensors for multimodal and quantitative sensing of mechanical deformations were developed based on distributed fiber-optic sensor systems.[79] The stretchable fiber optic sensors were constructed with a colored core doped with colorimetric dyes at four different locations and a transparent core embedded in silicone cladding. The mechanical deformations (stretch, press, bend, and twist) can induce geometric changes in the light propagation path and thus affect the chromaticity and intensity outputs. The fiber optic system realized the bending sensitivity of 7 to 24 dB cm^{-1} for different mechanical deformations and the bending resolution of 0.5°. Such fiber optic sensors were integrated into a 3D-printed soft glove (Figure 5b.i-ii). The wireless glove demonstrates multilocation decoupling and reconstruction of various types of finger joint

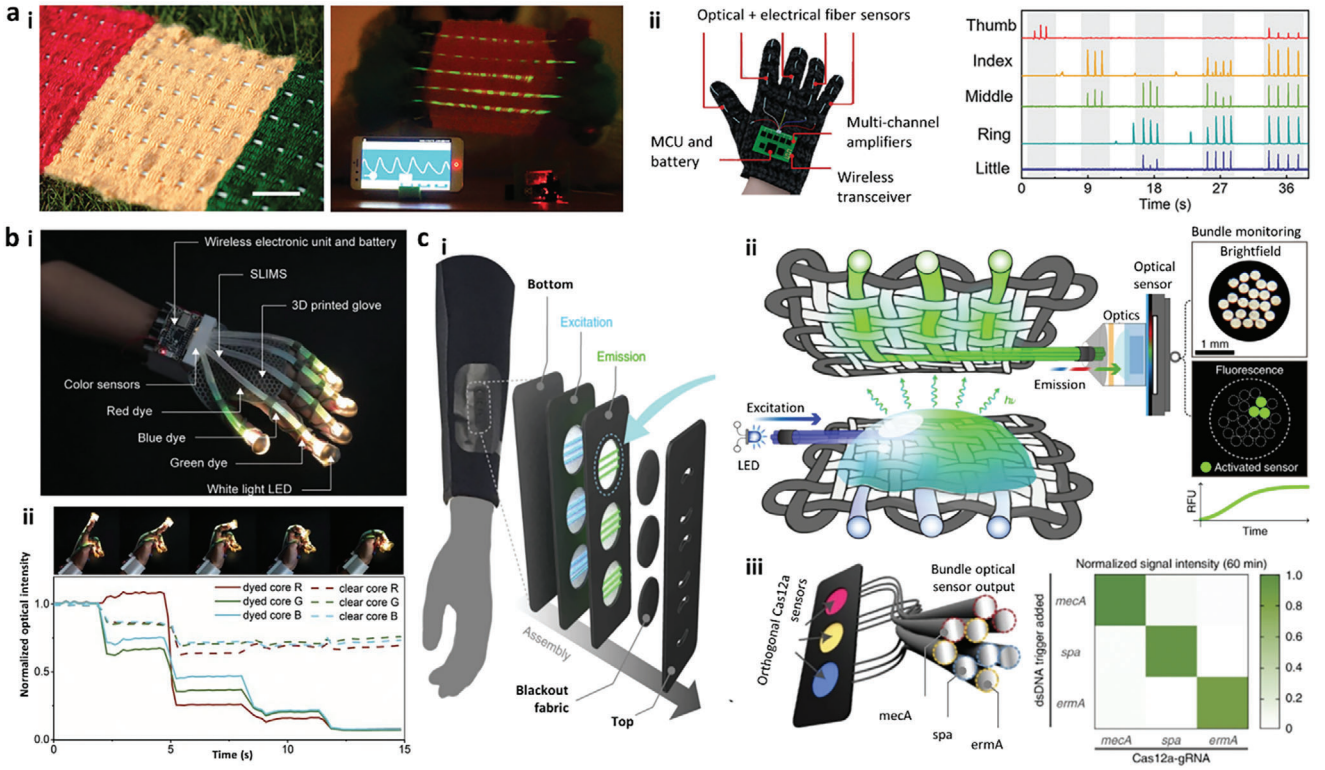

Figure 5. Wearable fiber optic sensor devices. a) Wearable textiles embedded by self-powered mechanical optoelectronic fiber sensors. i) photos of visual–digital synergies by the combination of optical and electrical outputs in the smart fiber and textile. ii) the fiber optics were knitted into a smart glove to simultaneously report optical and electrical signals for stress digitization. Adapted with permission from Wiley-VCH 2021.[76] b) Stretchable silica-based distributed fiber-optic sensors of mechanical deformation. i) integrated as a wireless 3D-printed glove with white light LED, battery, and electronics; ii) real-time monitoring of the optical intensity under five different multi-joint bending configurations. Adapted with permission from the American Association for the Advancement of Science 2020.[79] c) Synthetic biology wearables for biomolecule detection. i) textiles embedded with fiber optics allow excitation/emission light transmission and the detection of FDCF sensors. ii) inter-weaved POFs in the two layers of hydrophobically patterned fabrics are excited by LED arrays and the emission signals are collected via an optical fiber bundle, filter, and collimating lens. iii) multiplexed CRISPR-based wearable sensors and orthogonal detection of different sensors upon exposure to specific triggers. Adapted with permission from Springer Nature 2021.[80]

movements in real-time. The design of elastomeric light guides in fiber optics with chromatic patterns can be enhanced by high-resolution sensor chips and miniaturized by tapered fibers.

Recently, biomolecule detections by genetically encoded optical sensors have been realized and integrated into flexible substrates and wearables such as silicone elastomers, textiles, and face masks.[80] As robust synthetic biology reactions, the freeze-dried, cell-free (FDCF) genetic circuits are activated upon the rehydration through aqueous interactions and reflect the existence of chemicals, metabolites, nucleic acid, and SARS-CoV-2 via a fiber optic network (Figure 5c.i). The polymeric optic fibers (POFs) were inter-weaved and incorporated in textiles to embed PDCF reaction components and transmit the excitation (447 nm) and emission light (510 nm) for signal interrogation (Figure 5c.ii). All emissive POFs were bundled as a multiplexed optical sensor system with a filter and collimating lens for the generation of temporally and spatially resolved fluorescence images. Multiplexed CRISPR-based nucleic acid sensors[81] were integrated into the FDCF wearables and their orthogonal behaviors to specific dsDNA triggers were demonstrated, in which mecA sensor showed the single-digit femtomolar sensitivity of 2.7 fM. (Figure 5c.iii). In this work, the combination of synthetic biology sensors in fiber optics enables precise and multiplexed biomolecule detections. The optical outputs from different fiber optic sensors can be merged into a single bundle for centralized signal collection and analysis.

3.3. Implantable Sensors and Diagnostics

Optical waveguides to control and deliver light to target sites without any obstruction, especially in deep-region tissues and organs are highly desired for implantable light-based medical diagnostics.

To reduce the inflammation and discomfort of solid-state fibers, biocompatible cell-integrated PEG hydrogels have been developed for implantable sensing and therapy.[82] The hydrogel-based optical fibers were constructed by poly(acrylamide-co-poly(ethylene glycol) diacrylate) hydrogel (n = 1.46–1.50, thickness 0.2–2 mm) as the core and Ca alginate hydrogel (n = 1.339, thickness 50–100 µm) as the cladding layer, where the core was covalently functionalized by glucose-specific receptors.[83] The quantitative glucose monitoring results were collected by detecting the variations in the light transmission intensity through the

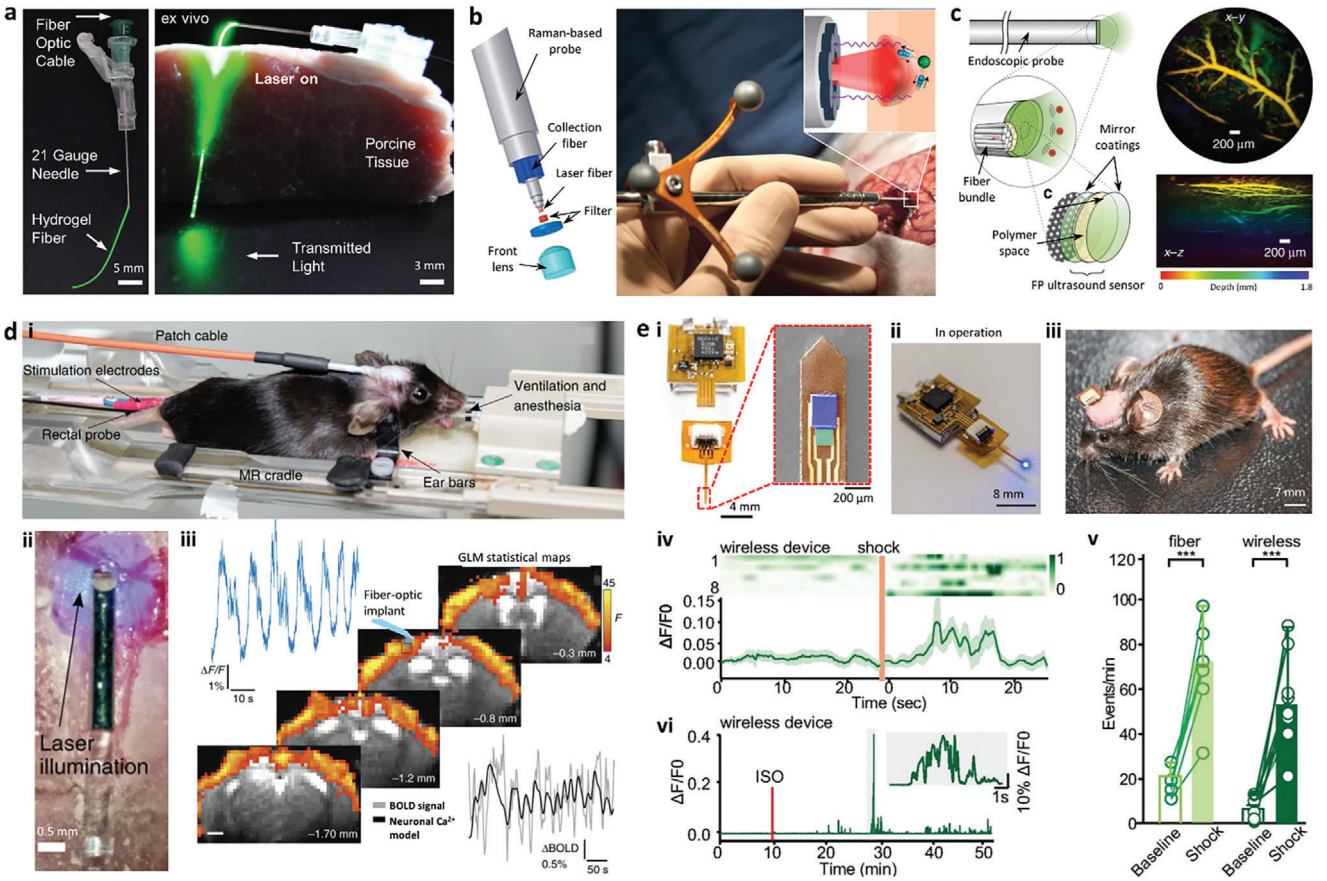

Figure 6. Implantable fiber optic sensor devices. a) Hydrogel optical fiber was connected with needles for interstitial fluid monitoring in porcine tissue as insertable devices as deep as 3 cm. Adapted with permission from Wiley-VCH 2017.[82] b) The handheld silica-based Raman fiber optic probe connected with a NIR laser, and a CCD spectroscopic detector was used to differentiate the Raman spectra of cancer and normal brain tissue. Adapted with permission from the American Association for the Advancement of Science 2015.[84] c) The distal end of the photoacoustic endoscopy probe shows the coherent fiber bundle with a subset of fiber-optic cores and the Fabry-Pérot ultrasound sensor constructed by two dielectric mirror coatings and a spacer layer. Photoacoustic images were taken at *x*–*y* and vertical *x*–*z* maximum intensity projections for mouse abdominal skin microvasculature. Adapted with permission from Springer Nature 2018.[86] d) i) The fiber-optic implant was embedded in the mouse head, which was covered with a dental composite layer and connected to the patch cable. ii) The light illumination of the brain surface was obtained through the reflection at a right-tip rotation angle via a mirror coating. iii) The measurement results of chronic simultaneous Ca^{2+} recording/BOLD fMRI monitoring under the resting-state conditions for 6 weeks post-implantation. Adapted with permission from Springer Nature 2018.[88] e) Miniaturized wireless photometry systems for Ca^{2+} detection in the deep brain. i) Optical graph of the injectable photometry probe with magnified colorized SEM image of the device tip. ii) The integrated transponder and injectable are in operation. iii) A living mouse with a photometry system was inserted for a week. iv) Heatmap before and after shock recorded by wireless device. v) Spike events frequency signals before (baseline) and after shock measured by fiber and wireless photometry systems. vi) Fluorescence trace showing injection of isoproterenol recorded by wireless photometry system. Adapted with permission from the National Academy of Sciences 2018.[91]

hydrogel optical fibers. Then the hydrogel fiber was incorporated with a syringe needle for injection, implantation, and retraction in porcine tissue as deep as 3 cm and controllable light transmission (**Figure 6a**). Intensity-based readout in this work is affected by light loss through bending, thus hydrogel fibers embedded with Bragg gratings for the changes in refractive index can improve the quantitative measurements.

With the aim to accurately detect cancer cells, a handheld intraoperative Raman spectroscopy probe for real-time recognition of brain cancer has been developed (Figure 6b).[84] The contact fiber optic-based Raman spectroscopy probe can illuminate a tissue area of 0.5 mm diameter with a depth of ≈1 mm for a total acquisition time of 0.2 s. Based on the Raman spectral comparisons between normal and cancer brain tissues due to their differences in cholesterol, phospholipids, and nucleic acid, the probe can achieve cancer detection with an accuracy of 92%, a sensitivity of 93%, and a specificity of 91%. This technology has the potential to enable the real-time classification of cell populations and evolve the neurosurgical workflow from current imaging techniques for surgical reSection.

Apart from spectroscopy-integrated fiber optics, optical imaging techniques such as light microscopy[85] and OCT[9] have been constructed in fiber optic systems to detect early-stage tissue abnormalities. Recently, a high-frequency OCT system with an imaging console and a fiber-optic endoscopic probe has been developed for rapid volumetric microscopy of cerebrovascular arteries.[86] In contrast to optical imaging, photoacoustic imaging using laser-generated ultrasound can provide deeper

penetration (up to 10 mm) and higher resolution along with a wide −3 dB bandwidth of 34 MHz.[87] A miniature forward-viewing photoacoustic imaging probe that integrated Fabry–Pérot ultrasound sensor at the tip of a fiber bundle has been constructed for high-resolution 3D endoscopy (Figure 6c).[88] With penetration depth ranging from 1 to 7 mm, high-resolution photoacoustic imaging was achieved. The 3D images of the microvascular anatomies in duck embryo and mouse skin tissues were demonstrated with remarkable image fidelity. This work paves a pathway for a new class of fiber optic photoacoustic probes for high-resolution imaging and endoscopic diagnostics.

Implantation of fiber optics allows for monitoring neural dynamics with cellular, anatomic, and temporal precision in freely moving animals with minimal damage to tissue.[89] A simple and sensitive method to record the neuronal activities in the deep brain tissue is fiber photometry, in which optical signals are activated from the coupled excitation light and collected from fluorescent indicators at the fiber tip.[90] Genetically encoded calcium indicators, like GCaMP fluorescent proteins, have been widely used for the fluorescent measurement of genetically defined neuronal activities. The fluorescent calcium indicator GCaMP6, which emits increasingly upon calcium binding, has been used for long-term measurement of calcium dynamics in the mouse brain through a chronically implanted optical fiber (Figure 6d.i).[91] The fiber-optic implant was directly inserted into the neocortex and freely repositioned for maximal intensity during the measurement (Figure 6d.ii). The bulk signals detected by fiber-optic implant enable the detection of spontaneous calcium signals over a period of weeks, which displays a strong correlation with blood oxygen level-dependent (BOLD) functional MRI (fMRI) (Figure 6d.iii).

Despite the effectiveness of the fiber-optic implant, the bulk fiber-optic cable can physically limit the recording of neural activity and associated motion artifacts. A light-weight and wireless fluorescence photometer integrated with a miniaturized light source and a photodetector have been constructed on the thin and flexible polymer support (Figure 6e.i-ii).[92] The minimally invasive insertion and stable chronic operation of the fiber-optic probe enable wireless stimulation of genetically encoded calcium indicators in the deep brain of freely moving animal models (Figure 6e.iii). The wireless fiber-optic implant presents a sensitive recording of calcium transients, stable data collection over large areas, and minimal interruption in natural behaviors (Figure 6e.iv-vi). High-density arrays of optical fibers (up to 24 fibers) were built for multi-fiber photometry to enable simultaneous measurement of large-scale brain circuit dynamics (up to 48 brain regions) in the mammalian brain.[93] Fiber photometry based on flat-cleaved optical fibers has been advanced by tapered optical fibers to enhance the light excitation and collection efficiency, where light collection over up to 2 mm of tissue along the fiber taper from multiple brain regions has been realized.[94] Remote detection via fiber photometry has emerged as a powerful technique in neuroscience research and shows great potential for minimally invasive diagnosis of widespread human activities.

4. Fiber Optic Light-based Treatments

Various photochemical and photobiological effects on biological systems have been known and implemented in clinical medicine as well as biomedical research. Furthermore, new techniques, such as optogenetics, have been developed, extending the scope of light-based manipulation of biological systems. In general, light offers advantages of spatiotemporal precision and molecular specificity through the control of wavelength, intensity, and light-responsive proteins via genetic incorporation. In this Section, we provide an overview of several major categories of light-based therapies and the roles that optical fibers play in each. We further highlight specific examples to showcase key innovations in optical fibers including novel use of waveguide principle, fabrication material, fabrication method, or device implementation, in each application category.

4.1. Optogenetics

Optogenetics is a technique that combines genetic and optical methods to manipulate cellular behavior, which generally follows a light-mediated mechanism as depicted in **Figure 7a**.[95,96] Briefly, light-activated proteins, e.g. channelrhodopsin (ChR) and halorhodopsin, are genetically encoded into cells. Desired light illumination with specified spatiotemporal resolution, wavelength, and location is then applied to manipulate the cells via either excitation of channelrhodopsin or inhibition of halorhodopsin. The resulting cellular activity can be then monitored by either genetically encoded sensors for ions or membrane voltage. Thanks to the development of various light-activated proteins, gene delivery strategies, light delivery methods, and measurement techniques for optogenetic readouts, this field has been involved very rapidly over the past decade, making optogenetics a widely used research tool to interrogate the neural circuitry for understanding various disease mechanisms. Optogenetics-based therapies have also shown exciting potential to treat diseases including retina diseases[97,98] and neurological disorders.[99–101] Although encouraging, light delivery issues, e.g. penetration depth, spatial precision, and accessibility to desired locations, still pose a fundamental challenge to this field thus limiting its full potential for both neuroscience research and therapeutic applications. To address these issues, fiber optic waveguides have been employed, considering their effectiveness, versatility, and minimal invasiveness by guiding light deep inside the brain.[102] Among them, several recent innovations in fiber optic devices, as we particularly highlighted below, have significantly advanced the field.

Conventional optogenetic interrogation relies on multiple separated and sequentially performed procedures that include light-activated opsin delivery, light delivery, and subsequent electrical recording. Recent work has demonstrated that the incorporation of all three procedures into a single miniature, flexible, all-polymer fiber device is feasible.[103,104] This multifunctional fiber device was designed to have six electrodes customized by graphite-loaded conductive polyethylene (gCPE) for neural signals transmission, two microfluidic channels for viral vector delivery, and a waveguide core made of polycarbonate (refractive index: 1.59) for light delivery and stimulation (Figure 7b,c). Its gCPE and microfluidic channels were arranged around the core and further separated by cyclic olefin copolymer-based cladding (refractive index, 1.53) so that the difference of

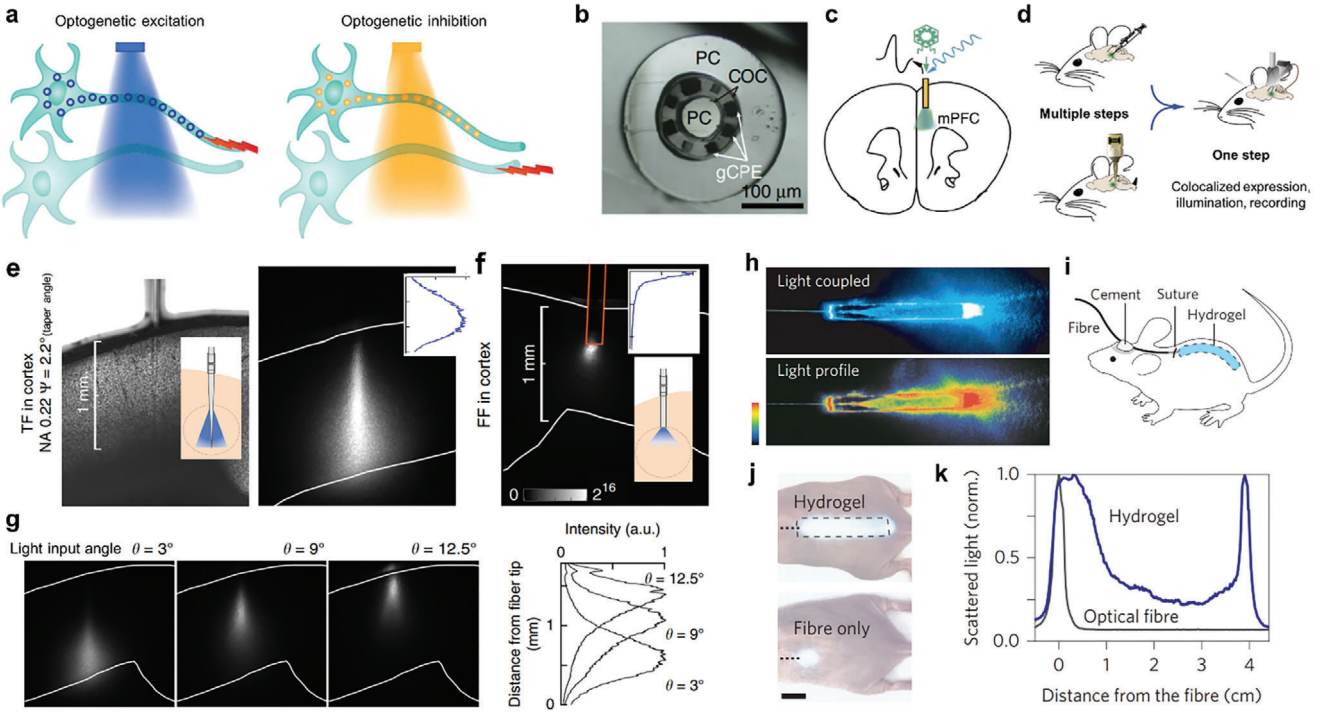

Figure 7. Applications of fiber-optic devices in optogenetics. a) General mechanism of optogenetics. Adapted with permission from Springer Nature 2011.[95] b) Cross–sectional view of multifunctional fiber device incorporating 6 recording electrodes, one optical waveguide core, and two microfluidic channels. PC, polycarbonate. COC, cyclic olefin copolymer. gCPE, graphite conductive polyethylene. c) Schematic of viral delivery, optical stimulation, and electrical recording in mice medial prefrontal cortex (mPFC) with the multifunctional fiber device. d) Schematic comparing a traditional optogenetic procedure with that of a multifunctional fiber device. Adapted with permission from Springer Nature 2017.[104] e) Brightfield image (left) showing the position of a tapered optical fiber (TF) implanted in a fluorescein-impregnated brain slice, inset showing a schematic of light delivery through TFs. Light-induced fluorescence from the implanted TF showing light emission intensity and distribution (right), inset showing normalized fluorescence intensity profile. f) Light-induced fluorescence from a flat-faced optical fiber (FF) in a fluorescein-impregnated brain slice with a top inset showing a normalized fluorescence intensity profile and a bottom inset showing a schematic of light delivery through FFs. g) Site-selective light delivery through TFs (NA = 0.22, $\Psi = 2.2°$) implanted into a fluorescent-stained mouse brain slice with light coupled at different input angles (3°, 9°, 12.5°) (left). Normalized fluorescence intensity profiles along depth starting from the tapered fiber end analyzed from the fluorescence images (right). Adapted with permission from Springer Nature 2017.[105] h) Image showing a light-coupling hydrogel (Top). Pseudo-color light distribution of the same hydrogel (bottom). i) Schematic of a fiber-pigtailed hydrogel implanted in a mouse. j) Images showing the light distribution of a hydrogel implant (top) and a convectional optical fiber (bottom). k) Axial light intensity plot from the hydrogel implant (blue) and conventional optical fiber (black). Adapted with permission from Springer Nature 2013.[82]

refractive indexes was sufficient to confine light within the core per principles in Section 2. Subsequently, all these components were incorporated into a macroscopic preform by standard machining, went through a thermal drawing process, and eventually achieved a small footprint with a diameter of 180–220 μm. As a result, this device enabled multiple simultaneous optogenetic procedures just after a one-step implantation surgery. This approach significantly simplified conventional optogenetic protocol and minimized tissue damage (Figure 7d). Its all-polymer composite design further reduced tissue response. These advantages collectively led to the opto-electrophysiological investigation of projections from the basolateral amygdala to the medial prefrontal cortex and ventral hippocampus during behavioral experiments.

In optogenetics, the precise control of neural processes highly depends on the spatiotemporal precision of light delivery. However, the spatial extent of light illumination within the brain is difficult to control or adjust using conventional fiber optics. Recently, a single tapered optical fiber coupled with reconfigurable emission was demonstrated to enable either large-area or spatially restricted illumination without the need to move the implant (inset in Figure 7e).[105] The tapered tip was designed and fabricated through laser heating-based thermal drawing of conventional MMF with precisely tunable taper angles and lengths. Starting from its proximal end, the injected light was guided toward its tip via total internal reflection with its propagation angle increased roughly by its taper angle at each reflection until total reflection was lost, at where light leaked from the fiber. The distance from this emitting position to the tapered tip was correlated with the fiber numerical aperture and light incident angle. Following this principle, light can be then guided for either large-area illumination by injecting light at the full numerical aperture or for spatially restricted illumination along the tapered tip by precisely tuning light input angle as demonstrated in fluorescein-impregnated mouse brain slices. Specifically, light delivered at full numerical aperture resulted in elongated (e.g., 1 mm) and relatively homogenous illumination along the tapered tip (Figure 7e), whereas convectional flat-faced optical fiber only

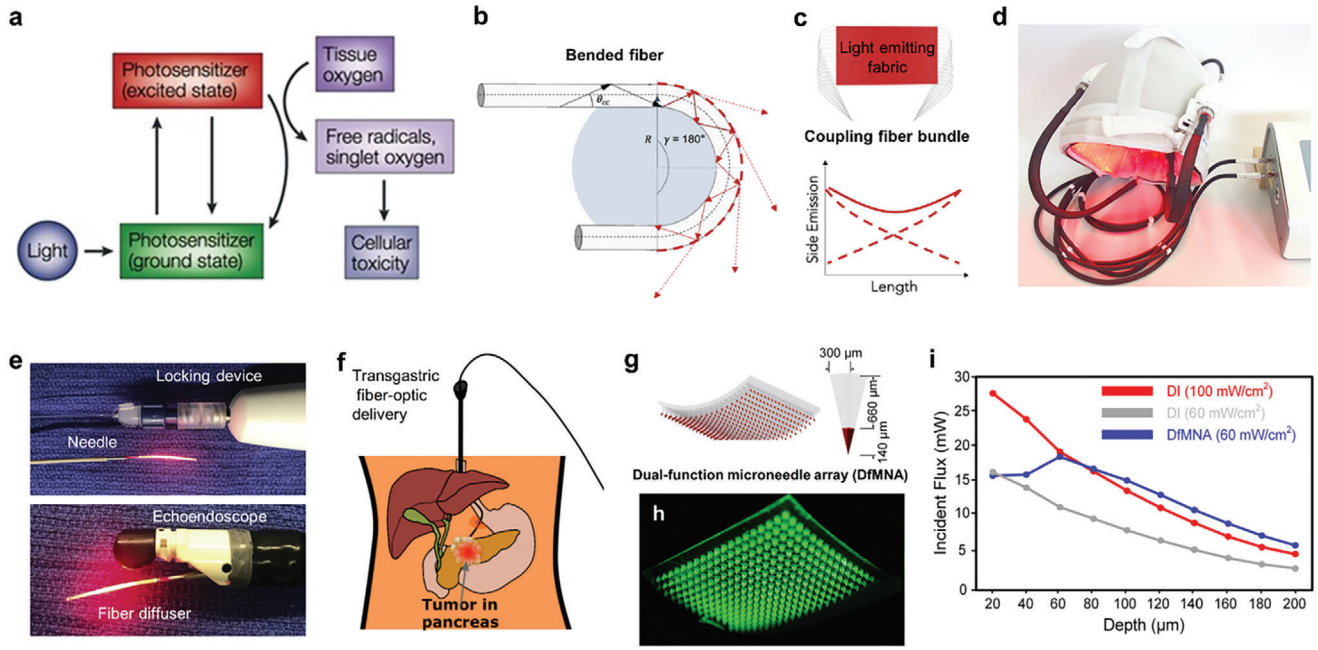

Figure 8. Applications of fiber-optic devices in photodynamic therapy. a) General mechanism of photodynamic therapy. Adapted with permission from Springer Nature 2003.[10] b) Principle of side-emitting optical fiber due to macro-bending. Solid arrow, confined light within fiber. Dashed arrow, leaked light. c) Top: schematic of light-emitting fabric with light coupling into two fiber bundles. Bottom, side-emitting intensity along the light-emitting fabric. Solid line, light coupled into both ends. Dashed red line, light coupled into one end. d) Image of light-emitting fabric-integrated helmet used for the treatment of actinic keratosis. Adapted with permission from Wiley-VCH 2020.[113] e) EUS-PDT device composed of a puncture needle, a fiber diffuser, a locking device for the puncture needle and fiber diffuser, and an echoendoscope. Adapted with permission from Elsevier Inc. 2019.[119] f) Trans-gastric fiber-optic delivery approach for EUS-PDT. g) Schematic of flexible dual-function microneedle array with an enlarged microneedle. The microneedle consisted of a photosensitizer-loaded tip and a transparent polyvinyl alcohol body. h) Light guiding effect (525 nm) by dual-function microneedle array after photosensitizer-loaded tip dissolved. i) Light intensity at different skin depths either under direct and topical illumination at 60/100 mW cm^{-2} or with microneedle array-guided illumination at 60 mW cm^{-2}. Adapted with permission from the Royal Society of Chemistry 2022.[127]

illuminated a few hundred micrometers close to its fiber end (Figure 7f). When the light was coupled only at a specified angle, site-selective illumination was achieved by simply tuning the input angle (e.g., at 3, 9, and 12.5° in Figure 7g).

For optogenetic therapy that requires further enlarged illumination area at cm^2 scales inside tissue or organ, the tapered fibers can no longer meet the need. Instead, implantable and biocompatible light-guiding hydrogels can be developed and employed as shown in Figure 7h.[82] Specifically, the hydrogel can be fabricated by molding and ultraviolet light-induced polymerization and cross–linking of PEGDA precursor solution supplemented with a photo-initiator (Irgacure). Its excellent optical transparency (0.23 dB cm^{-1} for optical loss), structural stability, and mechanical flexibility made it a viable optical waveguide implant. Once the light was coupled into the hydrogel by an optical-fiber pigtail, then passing through a diffraction region, it was dispersed nearly uniformly along the entire 40-mm hydrogel, with no >6 dB variation (Figure 7i–k). Whereas light delivered by an implanted MMF was limited to a small region (2–3 mm) near its fiber end. This result indicated a 40-fold increase in optogenetic therapy area when compared to conventional MMF. Its utility for optogenetic therapy was further demonstrated by subsequent subcutaneous implantation and optogenetic production of antidiabetic glucagon-like peptide-1 in diabetic mice (Figure 7i). Light-treated group with intraperitoneally injected glucose apparently showed improved glucose hemostasis when compared to the non-treated.

4.2. Photodynamic Therapy

Photodynamic therapy (PDT) is an established modality that combines light with a photosensitizer for treating various diseases, especially cancers.[10] In this modality, light at a specific wavelength is applied to excite the exogenously delivered photosensitizer to its excited state; it then returns to the ground state by transferring energy to tissue oxygen and generating highly cytotoxic reactive oxygen species (ROS), such as singlet oxygen and free radicals (**Figure 8**a). With clinical approval of a series of photosensitizers, PDT has become a valuable option for treating a number of cancers including skin, lung, esophagus, bladder, ovarian, and brain.[106,107,108] Nevertheless, its clinical efficacy is highly dependent on the effective co-delivery of photosensitizer and light to the targeted malignant cells or tissue. Due to the poor penetration depth of light in tissue, its current clinical applications are primarily limited to treating superficial conditions. To resolve this challenge, a few strategies have been demonstrated or adopted, including fiber optic delivery, near-infrared light, and upconversion nanoparticles.[109–111] Compared to other methods, fiber optics is still a popular and effective way to guide light either endoscopically or interstitially to reach deep tissue or internal

organs. For example, fiber-optic PDT endoscopy has been adopted in current clinical practice.[112] With novel biocompatible fiber materials and fiber devices emerging, more applications for PDT could be expected, especially for those highlighted below.

For many applications for treating skin disorders, large-area, uniform illumination is an essential requirement for PDT. Thus far, light-emitting fabrics comprised of side-emitting optical fibers have been regarded as a practical and effective way to meet this need. They are particularly tangible to be implemented as flexible, wearable devices. As an example, a PDT fabric has been developed by weaving plastic optical fibers into the textile structure and further demonstrated for large-area treatment of actinic keratosis in a clinical trial.[113,114] Its uniform light delivery was achieved by macrobending of these optical fibers, which broke their total internal reflection condition and purposely allowed partial light leakage from the fiber core. Such leakage took place when the fiber bending radius was less than its critical bending radius (Figure 8b). A fully knitted fabric with fibers bundled together for simultaneous light coupling at both ends achieved a more uniform emission profile when compared to that of single-end coupling (Figure 8c). With further incorporation inside an ergonomic helmet, this PDT fabric was further applied for the clinical treatment of actinic keratosis (Figure 8d). Noteworthy, other approaches for inducing fiber side emission are also available. These include adding scattering material into fibers,[115] inducing scattering microbubbles in fibers,[116] and creating micro perforation/notch on fiber cladding.[117,118]

For PDT treatment of cancers, especially pancreatic cancer, there is a pressing need to deliver light to targeted malignant tissue deep inside the human body. Although optical fiber-based percutaneous interstitial light delivery has been established for PDT, this approach requires a long fiber passage to reach the pancreas, thus making it challenging for clinical adoption. Taking advantage of the proximity of endoscope to pancreas, an endoscopic ultrasound-guided, fiber diffuser-based PDT, termed EUS-PDT, was demonstrated as a safe and effective treatment for advanced pancreatic cancer in clinical trials.[119,120,121] In this device, the light was first guided by a long conventional optical fiber, then coupled into a short cylindrical optical diffuser fused at the distal end of the guiding fiber, and eventually reached the pancreatic tissue where the optical diffuser was inserted (Figure 8e). The precise placement of the optical diffuser was achieved with the guidance of an echoendoscope and a locking device after its transgastric placement and the needle puncture procedure to create its access to pancreatic cancer (Figure 8e bottom and Figure 8f). This clinical study established the feasibility and safety of EUS-PDT procedures. A more recent clinical study using a newly developed photosensitizer, verteporfin, further showed its promise for treating locally advanced pancreatic cancer.[122]

For PDT treatment of skin disorders, e.g. actinic keratoses and epidermoid carcinoma, local transdermal co-delivery of photosensitizer and light is highly preferred to avoid side effects induced by systematic injection of photosensitizer as well as by topical application of high-intensity light. Earlier studies have suggested that a microneedle array can be applied either as a minimally invasive tool for local drug/photosensitizer delivery[123,124] or as a transdermal optical waveguide.[125,126] Interestingly, a recent study explored the possibility of integrating the dual functionalities into a single microneedle array platform for effective transdermal co-delivery of photosensitizer and light.[127] Its light guiding bodies were fabricated by molding a soft polymer, polyvinyl alcohol, and its photosensitizer (temoporfin)-loading tip was developed by sodium hyaluronate molding (Figure 8g). Once fully inserted into the skin, its photosensitizer-loading tips quickly dissolved into the deep skin layer, leaving the remaining transparent microneedle body in place to further guide PDT light into the same skin layer for treatment (Figure 8h). The application of this microneedle array with 60 mW cm^{-2} topical illumination achieved similar light intensity beneath the stratum corneum as that of direct topical illumination at 100 mW cm^{-2} (Figure 8i). With further validation of in vivo mice model of port-wine stains in terms of effectiveness and adverse effects, this co-delivery microneedle-based PDT has shown obvious benefits over conventional PDT.

4.3. Photobiomodulation

Photobiomodulation, previously known as low-level light therapy, uses red or near-infrared light at lower intensity levels to relieve pain, stimulate healing, and reduce inflammation.[128] These beneficial photobiological effects have been either clinically observed or preclinically reported over the past several decades. There are several widely hypothesized mechanisms to elucidate these effects.[129,130] Cytochrome C oxidase in mitochondria and calcium ion channels are currently regarded as primary light-sensitive chromophores, followed by light-induced increase of ATP, reactive oxygen species, and nitric oxide (**Figure 9a**). Because these mechanisms are still not well understood, the clinical applications of photobiomodulation have been controversial, and largely empirical. Nevertheless, significant advances have been achieved in the development of wearable devices for pain management,[131] wound healing,[128] and traumatic brain injury.[132] Among them, many utilize optical fibers as the essential means for their light delivery or illumination. As an example, a flexible luminous fabric was developed by weaving a large number of side-emitting polymer optical fibers with conventional cotton yarns for large-area low-level light therapy.[133] PMMA and fluorinated PMMA derivatives were used as core and cladding materials, respectively, for fiber fabrication. The fully woven luminous fabric is shown in Figure 9b. Its light emission was achieved by creating serials of V-shaped notches along the fibers (Figure 9b inset).[118] The light was then simultaneously coupled into both fiber ends to compensate for light attenuation along fibers, and two fabric layers were further overlayed together to achieve relatively uniform illumination. With its flexibility, uniform illumination, and safe human use, it has shown promising potential as a wearables for photobiomodulation applications.

4.4. Photochemical Cross–linking

Light-induced chemical cross–linking has widely been applied in biomaterial engineering, drug synthesis, and dental-composite curing. Photochemical tissue bonding (PTB) is one of its medical applications that involves using light and a photoactive dye

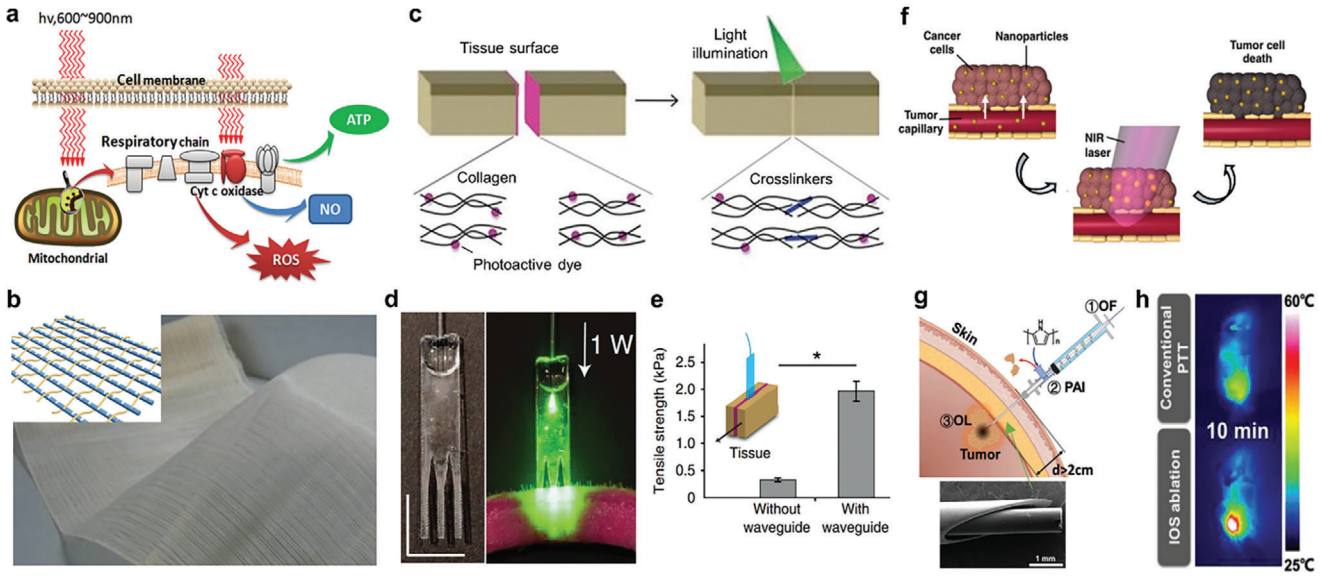

Figure 9. Applications of fiber-optic devices in other phototherapy approaches. a) Generally hypothesized mechanism of photobiomodulation. Adapted with permission from SAGE Publications Inc. 2011.[130] b) Image of flexible luminous fabrics produced from conventional cotton yarns and side-emitting polymer optical fibers. Zoom-in image showing a schematic of polymer optical fiber with V-shaped notches for side-emitting woven with cotton yarns. Adapted with permission from Optica Society 2013.[133] c) General mechanism of photochemical tissue bonding (PTB) or photochemical cross–linking. Adapted with permission from Elsevier B.V. 2016.[134] d) Left: biopolymer-based waveguide bundle designed for deep tissue illumination. Right: cross–section of the waveguide bundle inserted in porcine skin incision with light coupled for PTB activation. Adapted with permission from Springer Nature 2016.[12] e) Shear tensile strength after PTB in porcine skin with or without the waveguides. f) General mechanism of nanoparticle-based photothermal therapy. Adapted with permission from Wiley-VCH 2017.[135] g) Schematic of working principle of injectable optical system (IOS) for photothermal therapy. The IOS was composed of an optical fiber (OF), a photothermal agent (PAI), and an outlet (OL). Zoom-in: SEM image of the outlet with an inserted optical fiber. h) Thermal image of 4T1 tumor-bearing mice under conventional PPT and IOS-based PTT treatments. Adapted with permission from Wiley-VCH 2022.[136]

to bond two tissue surfaces together in a suture-less manner via light-mediated protein cross–linking. It has been demonstrated for wound closure, tissue grafting, and corneal/nerve repair.[137–139] The use of PTB is simple and straightforward (Figure 9c): photoactive dye solution is applied to tissue surfaces, which are then put in contact, followed by proper light illumination to induce sufficient protein crosslinkers for tissue bonding. However, as light has limited penetration depth in tissue, its application is primarily limited to superficial treatment (1–2 mm deep). One way to overcome this challenge is to develop a comb-shaped planar optical waveguide device as shown in Figure 9d (left) to be put between the two tissue surfaces.[12] It was designed to have both tapered legs and uniform Sections below for light guidance while having its edges on uniform Sections corrugated for light extraction. They were fabricated entirely by biocompatible and biodegradable polymers, e.g. polylactic acid, via a combination of molding, ultraviolet cross–linking, and laser cutting. As seen in Figure 9d (right), light in this device was first coupled via a pigtailed MMF, then guided into its uniform Sections via the tapered legs, and eventually scattered to surrounding tissue along the entire corrugated Sections. As demonstrated on porcine skin incision ex vivo, this device achieved a full thickness (>10 mm) and watertight wound closure, which represented a 10-fold extension of the bonded tissue area via conventional PTB (Figure 9d). Its bonding strength had also increased by >5-fold when compared with conventional PTB (Figure 9e). Besides PTB, photochemical cross–linking can also be used as "surgical glue" to repair vessel and heart defects, for which the activation light could be potentially delivered through optical fiber-based catheters.[140,141]

4.5. Photothermal Therapy

Photothermal therapy utilizes photothermal agent-induced heat for localized treatment of various medical conditions, especially cancers. During photothermal therapy, a photothermal agent is typically administrated and delivered to targeted tumor sites. After sufficient local accumulation in the tumor, a high-power NIR light is directly illuminated onto the tumor, so that light energy can be converted into local heat through the agent, subsequently leading to the death of tumor cells (Figure 9f).[135,142] Although some endogenous chromophores were initially used as the photothermal agent, their therapeutic effectiveness was weak, thus later replaced by these more effective, externally administrated agents, e.g. gold nanoparticles.[143–145] Recent clinical trials of gold nanoshells have shown their promising feasibility and effectiveness in treating prostate cancer.[146] Although encouraging, its treatment depth had been limited to several mm with topical NIR illumination. Among deep-tissue light delivery methods, optical fiber is still a minimally invasive, high-precision, more importantly, practical approach, which could be employed to resolve this issue. As an example, a recent work integrated photothermal agent administration, light delivery, and tissue

sampling simultaneously into a single MMF-based injectable optical system as illustrated in Figure 9g.[136,147] This system employed a modified syringe needle set and a conventional MMF, allowing the optical fiber to be guided by the needle and then inserted into the tumor for light delivery. Meanwhile, the interspace between the optical fiber and the needle was used for photothermal agent administration and subsequent passage of sampled tissue for biopsy analysis. Due to the efficient local co-delivery of photothermal agent and light, its treatment effectiveness was significantly improved when compared to conventional photothermal therapy (Figure 9h).

5. Conclusions and Outlook

Fiber optic technologies have been widely applied and shown a promising future in photomedicine for their efficient light delivery into internal organs and deep into tissues. The design and fabrication strategies of fiber optics or devices are driven by the specific needs of each sensing, diagnostics, and phototherapy application. The wide selection of compositing materials, scalable spatial precision, and easy device implementation led to the widespread adoption of optical fibers in photomedicine. The development of flexible, biocompatible, and biodegradable optical fiber materials is desired for safe and comfortable medical care applications.[148] Optical fibers fully based on biocompatible and bioresorbable materials are expected once their mechanical and optical performances are improved. The realization of multifunctional fiber bundles and mixed bundles is attracting more attention. The incorporation of 2D materials in optical fibers can promote the integration of photonic and optoelectronic systems for multimodal applications.[64] Tapered optical fibers have emerged recently as an attractive configuration out of standard fibers, to enhance the optical density and coupling efficiency between optical waveguide and functional materials.[149]

Recent advances in materials and fabrication techniques have promoted the development of multi-structural and multifunctional optical fibers. The lab-on-fiber technology to construct various architecture in light-matter interactions has established a remarkable platform for biomedical sensing. The remote modulation of multiplexed and dynamic optical signals via biophysical and biochemical stimuli is vital for next-generation diagnostic platforms.[150] By integrating photonic and microfluidics, optofluidic waveguide has emerged as a transformative optics device for light-manipulating, precise dynamic controlling, and high-performance sensing.[151] The incorporation of fiber optic sensors in wearable and implantable devices has shed light on remote and robust health monitoring at point-of-care and clinical settings. The combination of machine learning and artificial intelligence in fiber optical sensors can enhance the signal-to-noise ratio, fasten the signal readout process, facilitate data processing, and promote the development of multiplexed sensors by mitigating cross-sensitivity.[152] Particularly, an important direction is a multifunctional fiber-optic device that combines diagnosis with therapy in a single platform. Several other emerging phototherapy technologies may further require fiber optic-based device implementation. For example, blue light in the 400–470 nm range has shown great promise to be a drug-free broad-spectrum antimicrobial alternative.[153] This modality has the potential to treat various bacterial/fungal infections, yet to be clinically tested. Light-activated nanoparticle-based drug delivery is also emerging aiming for its on-demand, spatiotemporally controlled, or even personalized drug delivery.[154] This approach has been demonstrated in photodynamic therapy,[155] immunotherapy, gene therapy,[156] and stem cell differentiation.[157] Fiber optic-based light delivery could be utilized to facilitate drug release beyond the reach of topical light illumination. Given the versatile role of light in nature, more advanced fiber optic devices with diverse sensing, diagnosing, manipulating, and therapy abilities look very promising.

Acknowledgements

This work was funded by the U.S. Air Force Office of Scientific Research through grants FA9550-17-1-0277 (to S.H.Y.), FA9550-20-1-0063 (to S.H.Y.), and RSC enablement grant E22-8583590682 (to A.K.Y. and Y.H.).

Conflict of Interest

The authors declare no conflict of interest.

Author Contributions

A.K.Y. and S.Y. conceived the idea and initiated the work. Y.H. organized the discussions and major content. Y.H. P.M. and J.H. contributed equally to manuscript writing, mainly responsible for fiber optic sensors and health monitoring, materials, and fabrication, as well as light-based treatments, respectively. A.K.Y. and S.Y. guided the entire project and revised the manuscript.

Keywords

fiber optics, light waveguides, optical sensing, photomedicine, phototherapy

Received: February 20, 2024
Revised: May 4, 2024
Published online: June 25, 2024

[1] H. Jeong, W. Park, D. H. Kim, K. Na, *Adv. Drug Delivery Rev.* **2021**, *177*, 113954.
[2] J. M. Bae, H. M. Jung, B. Y Hong, J. H. Lee, W. J. Choi, J. H. Lee, G. M. Kim, *JAMA Dermatol* **2017**, *153*, 666.
[3] G. Wei, G. Yang, Y. Wang, H. Jiang, Y. Fu, G. Yue, R. Ju, *Theranostics* **2020**, *10*, 12241.
[4] A. Grzybowski, K. Pietrzak, *Clin. Dermatol.* **2012**, *30*, 451.
[5] A. F. McDonagh, L. A. Palma, D. A. Lightner, *Science* **1980**, *208*, 145.
[6] J. A. Parrish, T. B. Fitzpatrick, L. Tanenbaum, M. A. Pathak, *N. Engl. J. Med.* **1974**, *291*, 1207.
[7] L. De Chiffre, S. Carmignato, J. P. Kruth, R. Schmitt, A. Weckenmann, *CIRP Ann.* **2014**, *63*, 655.
[8] G. Iddan, G. Meron, A. Glukhovsky, P. Swain, *Nature* **2000**, *405*, 417.
[9] G. J. Tearney, M. E. Brezinski, B. E. Bouma, S. A. Boppart, C. Pitris, J. F. Southern, J. G. Fujimoto, *Science* **1997**, *276*, 2037.
[10] D. E. J. G. J. Dolmans, D. Fukumura, R. K. Jain, *Nat. Rev. Cancer* **2003**, *3*, 380.
[11] S. H. Yun, S. J. J. Kwok, *Nat. Biomed. Eng.* **2017**, *1*, 0008.

[12] S. Nizamoglu, M. C. Gather, M. Humar, M. Choi, S. Kim, K. S. Kim, S. K. Hahn, G. Scarcelli, M. Randolph, R. W. Redmond, S. H. Yun, *Nat. Commun.* **2016**, *7*, 10374.
[13] U. Utzinger, R. R. Richards-Kortum, *J. Biomed. Opt.* **2003**, *8*, 121.
[14] T. Vo-Dinh, *Biomedical photonics handbook: biomedical diagnostics*, CRC Press, USA **2014**.
[15] N. Rosenberg, A. C. Gelijns, H. Dawkins, *Sources of medical technology: universities and industry*, National Academy of Sciences, Washington, DC **1995**.
[16] W. E. Kelley Jr., *JSLS* **2008**, *12*, 351.
[17] S. Shabahang, S. Kim, S. H. Yun, *Adv. Funct. Mater.* **2018**, *28*, 1706635.
[18] S. Tabassum, R. Kumar, *Adv. Mater. Technol.* **2020**, *5*, 1900792.
[19] G. H. Lee, H. Moon, H. Kim, G. H. Lee, W. Kwon, S. Yoo, D. Myung, S. H. Yun, Z. Bao, S. K. Hahn, *Nat. Rev. Mater.* **2020**, *5*, 149.
[20] S. Young, *The Photonics Market Data and Industry Report 2020, Tematys and Photonics21,1 Photonics Public Private Partnership*, Oxford, UK, **2020**, 1–131.
[21] *The Medical Fiber Optics Market Size*, Precedence Research. WordPress, **2021**, Ottawa, Canada, 1221.
[22] *Light Therapy Market by End-user and Geographic Landscape – Forecast and Analysis*, Technavio,Toronto, Canada, **2021**.
[23] B. A. Flusbergc, E. D. Cocker, W. Piyawattanametha, J. C. Jung, E. L. M. Cheung, M. J. Schnitzer, *Nat. Methods* **2005**, *2*, 941.
[24] H. T. Zubair, M. Begum, F. Moradi, A. K. M. M. Rahman, G. A. Mahdiraji, A. Oresegun, G. T. Louay, N. Y. M. Omar, M. U. Khandaker, F. R. M. Adikan, N. M. Noor, K. S. Almugren, H. A. Abdul-Rashid, D. A. Bradley, *IEEE Photon. J.* **2020**, *12*, 1.
[25] P. Toupin, L. Brilland, J. Trolès, J. L. Adam, *Opt. Mater. Express* **2012**, *2*, 1359.
[26] P. Toupin, L. Brilland, C. Boussard-Plédel, B. Bureau, D. Mechin, J. L. Adam, J. Troles, *J. Non-Cryst. Solids* **2013**, *377*, 217.
[27] E. Ceci-Ginistrelli, D. Pugliese, N. G. Boetti, G. Novajra, A. Ambrosone, J. Lousteau, C. Vitale-Brovarone, S. Abrate, D. Milanese, *Opt. Mater. Express* **2016**, *6*, 2040.
[28] D. Gallichi-Nottiani, D. Pugliese, N. Giovanna Boetti, D. Milanese, D. Janner, *Int J Appl Glass Sci* **2020**, *11*, 632.
[29] R. Min, B. Ortega, C. Marques, *Photonics* **2019**, *6*, 36.
[30] X. Yue, H. Chen, H. Qu, R. Min, G. Woyessa, O. Bang, X. Hu, *Sensors* **2020**, *20*, 6643.
[31] D. Shan, C. Zhang, S. Kalaba, N. Mehta, G. B. Kim, Z. Liu, J. Yang, *Biomaterials* **2017**, *143*, 142.
[32] J. Feng, Q. Jiang, P. Rogin, P. W. de Oliveira, A. del Campo, *ACS Appl. Mater. Interfaces* **2020**, *12*, 20287.
[33] A. Gierej, A. Filipkowski, D. Pysz, R. Buczynski, M. Vagenende, P. Dubruel, H. Thienpont, T. Geernaert, F. Berghmans, *J. Light. Technol.* **2020**, *38*, 1905.
[34] M. B. Applegate, G. Perotto, D. L. Kaplan, F. G. Omenetto, *Biomed. Opt. Express* **2015**, *6*, 4221.
[35] L. Ma, Q. Liu, R. Wu, Z. Meng, A. Patil, R. Yu, Y. Yang, S. Zhu, X. Fan, C. Hou, Y. Li, W. Qiu, L. Huang, J. Wang, N. Lin, Y. Wan, J. Hu, X. Y. Liu, *Small* **2020**, *16*, 2000203.
[36] M. Choi, M. Humar, S. Kim, S. H. Yun, *Adv. Mater.* **2015**, *27*, 4081.
[37] J. Guo, X. Liu, N. Jiang, A. K. Yetisen, H. Yuk, C. Yang, A. Khademhosseini, X. Zhao, S. H. Yun, *Adv. Mater.* **2016**, *28*, 10244.
[38] G. Chen, K. Hou, N. Yu, P. Wei, T. Chen, C. Zhang, S. Wang, H. Liu, R. Cao, L. Zhu, B. S. Hsiao, M. Zhu, *Nat. Commun.* **2022**, *13*, 7789.
[39] E. A. Abou Neel, W. Chrzanowski, J. C. Knowles, *Acta Biomater.* **2008**, *4*, 523.
[40] A. Hoppe, N. S. Güldal, A. R. Boccaccini, *Biomaterials* **2011**, *32*, 2757.
[41] D. Pugliese, M. Konstantaki, I. Konidakis, E. Ceci-Ginistrelli, N. G. Boetti, D. Milanese, S. Pissadakis, *Opt. Lett.* **2018**, *43*, 671.
[42] D. Pugliese, N. G. Boetti,D. Janner, D. Milanese, in *Ceramics, Glass, and Glass-Ceramics*, Springer, Netherlands **2021**, 229.
[43] J. Zubia, J. Arrue, *Opt. Fiber Technol.* **2001**, *7*, 101.
[44] L. Bilro, N. Alberto, J. L. Pinto, R. Nogueira, *Sensors* **2012**, *12*, 12184.
[45] J. M. Anderson, M. S. Shive, *Adv. Drug Delivery Rev.* **1997**, *28*, 5.
[46] R. Fu, W. Luo, R. Nazempour, D. Tan, H. Ding, K. Zhang, L. Yin, J. Guan, X. Sheng, *Adv. Opt. Mater.* **2018**, *6*, 1700941.
[47] A. Dupuis, N. Guo, Y. Gao, N. Godbout, S. Lacroix, C. Dubois, M. Skorobogatiy, *Opt. Lett.* **2007**, *32*, 109.
[48] H. Orelma, A. Hokkanen, I. Leppänen, K. Kammiovirta, M. Kapulainen, A. Harlin, *Cellulose* **2020**, *27*, 1543.
[49] B. D. Lawrence, M. Cronin-Golomb, I. Georgakoudi, D. L. Kaplan, F. G. Omenetto, *Biomacromolecules* **2008**, *9*, 1214.
[50] H. Tao, J. M. Kainerstorfer, S. M. Siebert, E. M. Pritchard, A. Sassaroli, B. J. Panilaitis, M. A. Brenckle, J. J. Amsden, J. Levitt, S. Fantini, *PNAS* **2012**, *109*, 19584.
[51] E. Colusso, F. De Ferrari, P. Minzioni, A. Martucci, Y. Wang, F. G. Omenetto, *J. Mater. Chem. C* **2018**, *6*, 966.
[52] S. K. Hahn, J. K. Park, T. Tomimatsu, T. Shimoboji, *Int. J. Biol. Macromol.* **2007**, *40*, 374.
[53] N. Jiang, R. Ahmed, A. A. Rifat, J. Guo, Y. Yin, Y. Montelongo, H. Butt, A. K. Yetisen, *Adv. Opt. Mater.* **2018**, *6*, 1701118.
[54] D. T. Schaafsma, R. Mossadegh, J. S. Sanghera, I. D. Aggarwal, J. M. Gilligan, N. H. Tolk, M. Luce, R. Generosi, P. Perfetti, A. Cricenti, G. Margaritondo, *Ultramicroscopy* **1999**, *77*, 77.
[55] V. M. Sglavo, D. Pugliese, F. Sartori, N. G. Boetti, E. Ceci-Ginistrelli, G. Franco, D. Milanese, *J. Alloys Compd.* **2019**, *778*, 410.
[56] Y. Wang, Y. Huang, H. Bai, G. Wang, X. Hu, S. Kumar, R. Min, *Biosensors* **2021**, *11*, 472.
[57] K. Kong, C. Kendall, N. Stone, I. Notingher, *Adv. Drug Delivery Rev.* **2015**, *89*, 121.
[58] G. von Maltzahn, J. H. Park, K. Y. Lin, N. Singh, C. Schwöppe, R. Mesters, W. E. Berdel, E. Ruoslahti, M. J. Sailor, S. N. Bhatia, *Nat. Mater.* **2011**, *10*, 545.
[59] G. Kostovski, P. R. Stoddart, A. Mitchell, *Adv. Mater.* **2014**, *26*, 3798.
[60] J. I. Peterson, G. G. Vurek, *Science* **1984**, *224*, 123.
[61] Q. Wang, L. Wang, *Nanoscale* **2020**, *12*, 7485.
[62] R. Correia, S. James, S. W. Lee, S. P. Morgan, S. Korposh, *J Opt* **2018**, *20*, 073003.
[63] B. Kaur, S. Kumar, B. K. Kaushik, *Biosens. Bioelectron.* **2022**, *197*, 113805.
[64] J. H. Chen, Y. F. Xiong, F. Xu, Y. Q. Lu, *Light Sci Appl* **2021**, *10*, 1.
[65] P. Vaiano, B. Carotenuto, M. Pisco, A. Ricciardi, G. Quero, M. Consales, A. Crescitelli, E. Esposito, A. Cusano, *Laser Photonics Rev.* **2016**, *10*, 922.
[66] A. Ricciardi, A. Crescitelli, P. Vaiano, G. Quero, M. Consales, M. Pisco, E. Esposito, A. Cusano, *Analyst* **2015**, *140*, 8068.
[67] P. Russell, *Science* **2003**, *299*, 358.
[68] J. C. Knight, *Nature* **2003**, *424*, 847.
[69] X. Fan, I. M. White, *Nat. Photonics* **2011**, *5*, 591.
[70] G. Cui, S. B. Jun, X. Jin, G. Luo, M. D. Pham, D. M. Lovinger, S. S. Vogel, R. M. Costa, *Nat. Protoc.* **2014**, *9*, 1213.
[71] Z. Yang, T. Albrow-Owen, W. Cai, T. Hasan, *Science* **2021**, *371*, eabe0722.
[72] M. A. Pérez, O. González, J. R. Arias, M. A. Pérez, O. González, J. R. Arias, *Optical fiber sensors for chemical and biological measurements, Current Developments in Optical Fiber Technology*, Intech Open, Rijeka, Croatia **2013**, pp. 265–291.
[73] C. C. Jung, E. W. Saaski, D. A. McCrae, B. M. Lingerfelt, G. P. Anderson, *IEEE Sens. J.* **2003**, *3*, 352.
[74] E. W. Saaski, in *Frontiers in Pathogen Detection: From Nanosensors to Systems*, SPIE, USA, 32, **2009**.

[75] J. Kim, A. S. Campbell, B. E. F. de Ávila, J. Wang, *Nat. Biotechnol.* **2019**, *37*, 389.
[76] W. Yang, W. Gong, W. Gu, Z. Liu, C. Hou, Y. Li, Q. Zhang, H. Wang, *Adv. Mater.* **2021**, *33*, 2104681.
[77] K. Dong, X. Peng, R. Cheng, C. Ning, Y. Jiang, Y. Zhang, Z. L. Wang, *Adv. Mater.* **2022**, 2109355.
[78] M. Liu, X. Pu, C. Jiang, T. Liu, X. Huang, L. Chen, C. Du, J. Sun, W. Hu, Z. L. Wang, *Adv. Mater.* **2017**, *29*, 1703700.
[79] H. Bai, S. Li, J. Barreiros, Y. Tu, C. R. Pollock, R. F. Shepherd, *Science* **2020**, *370*, 848.
[80] P. Q. Nguyen, L. R. Soenksen, N. M. Donghia, N. M. Angenent-Mari, H. de Puig, A. Huang, R. Lee, S. Slomovic, T. Galbersanini, G. Lansberry, H. M. Sallum, E. M. Zhao, J. B. Niemi, J. J. Collins, *Nat. Biotechnol.* **2021**, *39*, 1366.
[81] J. S. Gootenberg, O. O. Abudayyeh, J. W. Lee, P. Essletzbichler, A. J. Dy, J. Joung, V. Verdine, N. Donghia, N. M. Daringer, C. A. Freije, C. Myhrvold, R. P. Bhattacharyya, J. Livny, A. Regev, E. V. Koonin, D. T. Hung, P. C. Sabeti, J. J. Collins, F. Zhang, *Science* **2017**, *356*, 438.
[82] M. Choi, J. W. Choi, S. Kim, S. Nizamoglu, S. K. Hahn, S. H. Yun, *Nat. Photonics* **2013**, *7*, 987.
[83] A. K. Yetisen, N. Jiang, A. Fallahi, Y. Montelongo, G. U. Ruiz-Esparza, A. Tamayol, Y. S. Zhang, I. Mahmood, S.-A. Yang, K. S. Kim, H. Butt, A. Khademhosseini, S. H. Yun, *Adv. Mater.* **2017**, *29*, 1606380.
[84] M. Jermyn, K. Mok, J. Mercier, J. Desroches, J. Pichette, K. Saint-Arnaud, L. Bernstein, M. C. Guiot, K. Petrecca, F. Leblond, *Sci. Transl. Med.* **2015**, *7*, 274ra219.
[85] W. Bishara, U. Sikora, O. Mudanyali, T. W. Su, O. Yaglidere, S. Luckhart, A. Ozcan, *Lab Chip* **2011**, *11*, 1276.
[86] G. J. Ughi, M. G. Marosfoi, R. M. King, J. Caroff, L. M. Peterson, B. H. Duncan, E. T. Langan, A. Collins, A. Leporati, S. Rousselle, D. K. Lopes, M. J. Gounis, A. S. Puri, *Nat. Commun.* **2020**, *11*, 3851.
[87] L. V. Wang, J. Yao, *Nat. Methods* **2016**, *13*, 627.
[88] R. Ansari, E. Z. Zhang, A. E. Desjardins, P. C. Beard, *Light Sci Appl* **2018**, *7*, 75.
[89] D. R. Sparta, A. M. Stamatakis, J. L. Phillips, N. Hovelsø, R. van Zessen, G. D. Stuber, *Nat. Protoc.* **2012**, *7*, 12.
[90] G. Cui, S. B. Jun, X. Jin, M. D. Pham, S. S. Vogel, D. M. Lovinger, R. M. Costa, *Nature* **2013**, *494*, 238.
[91] F. Schlegel, Y. Sych, A. Schroeter, J. Stobart, B. Weber, F. Helmchen, M. Rudin, *Nat. Protoc.* **2018**, *13*, 840.
[92] L. Lu, P. Gutruf, L. Xia, D. L. Bhatti, X. Wang, A. Vazquez-Guardado, X. Ning, X. Shen, T. Sang, R. Ma, *PNAS* **2018**, *115*, E1374.
[93] Y. Sych, M. Chernysheva, L. T. Sumanovski, F. Helmchen, *Nat. Methods* **2019**, *16*, 553.
[94] F. Pisano, M. Pisanello, S. J. Lee, J. Lee, E. Maglie, A. Balena, L. Sileo, B. Spagnolo, M. Bianco, M. Hyun, M. De Vittorio, B. L. Sabatini, F. Pisanello, *Nat. Methods* **2019**, *16*, 1185.
[95] K. O. Deisseroth, *Nat. Methods* **2011**, *8*, 26.
[96] K. Deisseroth, *Nat. Neurosci.* **2015**, *18*, 1213.
[97] J. A. Sahel, B. Roska, *Annu. Rev. Neurosci.* **2013**, *36*, 467.
[98] J. A. Sahel, E. Boulanger-Scemama, C. Pagot, A. Arleo, F. Galluppi, J. N. Martel, S. D. Esposti, A. Delaux, J. B. de Saint Aubert, C. de Montleau, E. Gutman, I. Audo, J. Duebel, S. Picaud, D. Dalkara, L. Blouin, M. Taiel, B. Roska, *Nat. Med.* **2021**, *27*, 1223.
[99] J. D. Ordaz, W. Wu, X. M. Xu, *Neural Regener. Res.* **2017**, *12*, 1197.
[100] S. Valverde, M. Vandecasteele, C. Piette, W. Derousseaux, G. Gangarossa, A. Aristieta Arbelaiz, J. Touboul, B. Degos, L. Venance, *Nat. Commun.* **2020**, *11*, 1.
[101] M. Creed, V. J. Pascoli, C. Lüscher, *Science* **2015**, *347*, 659.
[102] M. R. Warden, J. A. Cardin, K. Deisseroth, *Annu. Rev. Biomed. Eng.* **2014**, *16*, 103.
[103] A. Canales, X. Jia, U. P. Froriep, R. A. Koppes, C. M. Tringides, J. Selvidge, C. Lu, C. Hou, L. Wei, Y. Fink, P. Anikeeva, *Nat. Biotechnol.* **2015**, *33*, 277.
[104] S. Park, Y. Guo, X. Jia, H. K. Choe, B. Grena, J. Kang, J. Park, C. Lu, A. Canales, R. Chen, Y. S. Yim, G. B. Choi, Y. Fink, P. Anikeeva, *Nat. Neurosci.* **2017**, *20*, 612.
[105] F. Pisanello, G. Mandelbaum, M. Pisanello, I. A. Oldenburg, L. Sileo, J. E. Markowitz, R. E. Peterson, A. Della Patria, T. M. Haynes, M. S. Emara, B. Spagnolo, S. R. Datta, M. De Vittorio, B. L. Sabatini, *Nat. Neurosci.* **2017**, *20*, 1180.
[106] S. Kwiatkowski, B. Knap, D. Przystupski, J. Saczko, E. Kędzierska, K. Knap-Czop, J. Kotlińska, O. Michel, K. Kotowski, J. Kulbacka, *Biomed. Pharmacother.* **2018**, *106*, 1098.
[107] P. Agostinis, K. Berg, K. A. Cengel, T. H. Foster, A. W. Girotti, S. O. Gollnick, S. M. Hahn, M. R. Hamblin, A. Juzeniene, D. Kessel, *CA Cancer J Clin* **2011**, *61*, 250.
[108] M. T. Wan, J. Y. Lin, *Clin. Cosmet. Investig. Dermatology.* **2014**, *7*, 145.
[109] P. Chinna Ayya Swamy, G. Sivaraman, R. N. Priyanka, S. O. Raja, K. Ponnuvel, J. Shanmugpriya, A. Gulyani, *Coord. Chem. Rev.* **2020**, *411*, 213233.
[110] Y. Yang, Q. Guo, H. Chen, Z. Zhou, Z. Guo, Z. Shen, *Chem. Commun.* **2013**, *49*, 3940.
[111] N. M. Idris, M. K. Gnanasammandhan, J. Zhang, P. C. Ho, R. Mahendran, Y. Zhang, *Nat. Med.* **2012**, *18*, 1580.
[112] B. F. Overholt, M. Panjehpour, J. M. Haydek, *Gastrointest Endosc* **1999**, *49*, 1.
[113] S. Mordon, E. Thécua, L. Ziane, F. Lecomte, P. Deleporte, G. Baert, A. S. Vignion-Dewalle, *TBIO* **2020**, *2*, e202000005.
[114] A. S. Vignion-Dewalle, H. Abi Rached, E. Thecua, F. Lecomte, P. Deleporte, H. Béhal, T. Hommel, A. Duhamel, R. M. Szeimies, L. Mortier, S. Mordon, *JMIR Res Protoc* **2019**, *8*, e12990.
[115] J. Xu, Y. Ao, D. Fu, J. Lin, Y. Lin, X. Shen, C. Yuan, Z. Yin, *J Photochem Photobiol A Chem* **2008**, *199*, 165.
[116] S. Shabahang, S. Forward, S. H. Yun, *Opt. Express* **2019**, *27*, 7560.
[117] V. Koncar, *Opt Photonics News* **2005**, *16*, 40.
[118] J. Shen, X. Tao, D. Ying, C. Hui, G. Wang, *Text. Res. J.* **2013**, *83*, 730.
[119] J. M. DeWitt, K. Sandrasegaran, B. O'Neil, M. G. House, N. J. Zyromski, A. Sehdev, S. M. Perkins, J. Flynn, L. McCranor, S. Shahda, *Gastrointest Endosc* **2019**, *89*, 390.
[120] H. H. Chan, N. S. Nishioka, M. Mino, G. Y. Lauwers, W. P. Puricelli, K. N. Collier, W. R. Brugge, *Gastrointest Endosc* **2004**, *59*, 95.
[121] J. H. Choi, D. Oh, J. H. Lee, J. H. Park, K. P. Kim, S. S. Lee, Y. J. Lee, Y. S. Lim, T. J. Song, S. S. Lee, *Endoscopy* **2015**, *47*, 1035.
[122] Y. Hanada, S. P. Pereira, B. Pogue, E. V. Maytin, T. Hasan, B. Linn, T. Mangels-Dick, K. K. Wang, *Gastrointest Endosc* **2021**, *94*, 179.
[123] D. Li, D. Hu, H. Xu, H. K. Patra, X. Liu, Z. Zhou, J. Tang, N. Slater, Y. Shen, *Biomaterials* **2021**, *264*, 120410.
[124] R. F. Donnelly, D. I. J. Morrow, M. T. C. McCrudden, A. Z. Alkilani, E. M. Vicente-Pérez, C. O'Mahony, P. González-Vázquez, P. A. McCarron, A. D. Woolfson, *Photochem. Photobiol.* **2014**, *90*, 641.
[125] M. Kim, J. An, K. S. Kim, M. Choi, M. Humar, S. J. J. Kwok, T. Dai, S. H. Yun, *Biomed. Opt. Express* **2016**, *7*, 4220.
[126] X. Wu, J. Park, S. Y. A. Chow, M. C. Z. Kasuya, Y. Ikeuchi, B. Kim, *Biomed. Opt. Express* **2022**, *13*, 1045.
[127] H. Zhao, X. Wang, Z. Geng, N. Liang, Q. Li, X. Hu, Z. Wei, *Lab Chip* **2022**, *22*, 4521.
[128] H. Chung, T. Dai, S. K. Sharma, Y. Y. Huang, J. D. Carroll, M. R. Hamblin, *Ann. Biomed. Eng.* **2012**, *40*, 516.
[129] L. F. de Freitas, M. R. Hamblin, *IEEE J. Sel. Top. Quantum Electron.* **2016**, *22*, 348.
[130] Y. Y. Huang, K. Sharma, J. Carroll, M. R. Hamblin, Biphasic dose response in low-level light therapy–an update. Dose-response 9, dose-response. 11-009. Hamblin, **2011**.
[131] R. T. Chow, M. I. Johnson, R. A. Lopes-Martins, J. M. Bjordal, *Lancet* **2009**, *374*, 1897.

[132] M. A. Naeser, R. Zafonte, M. H. Krengel, P. I. Martin, J. Frazier, M. R. Hamblin, J. A. Knight, W. P. Meehan, E. H. Baker, *J Neurotrauma* **2014**, *31*, 1008.
[133] J. Shen, C. Chui, X. Tao, *Biomed. Opt. Express* **2013**, *4*, 2925.
[134] M. Ark, P. H. Cosman, P. Boughton, C. R. Dunstan, *Int. J. Adhes. Adhes.* **2016**, *71*, 87.
[135] R. S. Riley, E. S. Day, *Wiley Interdiscip Rev Nanomed Nanobiotechnol* **2017**, *9*, e1449.
[136] Y. Ma, Y. Chu, S. Lyu, Y. He, Y. Wang, *Adv. Mater. Technol.* **2022**, *7*, 2101464.
[137] T. S. Johnson, A. C. O'Neill, P. M. Motarjem, C. Amann, T. Nguyen, M. A. Randolph, J. M. Winograd, I. E. Kochevar, R. W. Redmond, *J. Surg. Res.* **2007**, *143*, 224.
[138] B. P. Chan, I. E. Kochevar, R. W. Redmond, *J. Surg. Res.* **2002**, *108*, 77.
[139] Y. Kamegaya, W. A. Farinelli, A. V. Vila Echague, H. Akita, J. Gallagher, T. J. Flotte, R. R. Anderson, R. W. Redmond, I. E. Kochevar, *Lasers Surg Med* **2005**, *37*, 264.
[140] E. T. Roche, A. Fabozzo, Y. Lee, P. Polygerinos, I. Friehs, L. Schuster, W. Whyte, A. M. Casar Berazaluce, A. Bueno, N. Lang, M. J. N. Pereira, E. Feins, S. Wasserman, E. D. O'Cearbhaill, N. V. Vasilyev, D. J. Mooney, J. M. Karp, P. J. del Nido, C. J. Walsh, *Sci. Transl. Med.* **2015**, *7*, 306ra149.
[141] N. Lang, M. J. Pereira, Y. Lee, I. Friehs, N. V. Vasilyev, E. N. Feins, K. Ablasser, E. D. O'Cearbhaill, C. Xu, A. Fabozzo, R. Padera, S. Wasserman, F. Freudenthal, L. S. Ferreira, R. Langer, J. M. Karp, P. J. del Nido, *Sci. Transl. Med.* **2014**, *6*, 218ra216.
[142] J. R. Melamed, R. S. Edelstein, E. S. Day, *ACS Nano* **2015**, *9*, 6.
[143] S. Lal, S. E. Clare, N. J. Halas, *Acc. Chem. Res.* **2008**, *41*, 1842.
[144] L. Zou, H. Wang, B. He, L. Zeng, T. Tan, H. Cao, X. He, Z. Zhang, S. Guo, Y. Li, *Theranostics* **2016**, *6*, 762.
[145] H. S. Jung, P. Verwilst, A. Sharma, J. Shin, J. L. Sessler, J. S. Kim, *Chem. Soc. Rev.* **2018**, *47*, 2280.
[146] A. R. Rastinehad, H. Anastos, E. Wajswol, J. S. Winoker, J. P. Sfakianos, S. K. Doppalapudi, M. R. Carrick, C. J. Knauer, B. Taouli, S. C. Lewis, A. K. Tewari, J. A. Schwartz, S. E. Canfield, A. K. George, J. L. West, N. J. Halas, *Proc. Natl. Acad. Sci. USA* **2019**, *116*, 18590.
[147] Y. Ran, Z. Xu, M. Chen, W. Wang, Y. Wu, J. Cai, J. Long, Z. S. Chen, D. Zhang, B.-O. Guan, *Adv. Sci. (Weinh)* **2022**, *9*, 2200456.
[148] C. F. Guimarães, R. Ahmed, A. Mataji-Kojouri, F. Soto, J. Wang, S. Liu, T. Stoyanova, A. P. Marques, R. L. Reis, U. Demirci, *Adv. Mater.* **2021**, *33*, 2105361.
[149] J. Xiao, T. Zhou, N. Yao, S. Ma, C. Pan, P. Wang, H. Fu, H. Liu, J. Pan, L. Yu, S. Wang, *Nat. Commun.* **2022**, 1.
[150] Y. Zhang, Y. Hu, Q. Liu, K. Lou, S. Wang, N. Zhang, N. Jiang, A. K. Yetisen, *Matter* **2022**, *5*, 3937.
[151] V. Ganjalizadeh, G. G. Meena, T. A. Wall, M. A. Stott, A. R. Hawkins, H. Schmidt, *Nat. Commun.* **2022**, *13*, 1035.
[152] A. Venketeswaran, N. Lalam, J. Wuenschell, P. R. Ohodnicki, M. Badar, K. P. Chen, P. Lu, Y. Duan, B. Chorpening, M. Buric, *Adv Intell Syst* **2022**, *4*, 2100067.
[153] Y. Wang, Y. Wang, Y. Wang, C. K. Murray, M. R. Hamblin, D. C. Hooper, T. Dai, *Drug Resist Updat* **2017**, *33*, 1.
[154] Y. Tao, H. F. Chan, B. Shi, M. Li, K. W. Leong, *Adv. Funct. Mater.* **2020**, *30*, 2005029.
[155] B. Q. Spring, R. Bryan Sears, L. Z. Zheng, Z. Mai, R. Watanabe, M. E. Sherwood, D. A. Schoenfeld, B. W. Pogue, S. P. Pereira, E. Villa, T. Hasan, *Nat. Nanotechnol.* **2016**, *11*, 378.
[156] I. A. Shestopalov, S. Sinha, J. K. Chen, *Nat. Chem. Biol.* **2007**, *3*, 650.
[157] J. Li, W. Y. W. Lee, T. Wu, J. Xu, K. Zhang, D. S. Hong Wong, R. Li, G. Li, L. Bian, *Biomaterials* **2016**, *110*, 1.

Yubing Hu is a Research Associate and Assistant PhD Supervisor in the Department of Chemical Engineering at Imperial College London. Dr. Hu received a bachelor's degree from Zhejiang University in 2016 and earned a PhD degree from the Hong Kong University of Science and Technology in 2020. She is experienced in organic synthesis, functional polymer materials, optical sensing, and analytical devices. With an aim to innovate healthcare technologies and translate them into individualized medications, she is highly motivated to develop optical biosensors and biomedical devices for portable, wearable, and implantable diagnostics and therapeutics.

Paolo Minzioni is an Associate Professor at the University of Pavia, School of Engineering. His main research activity is in the field of integrated photonics, with two separate focus areas. One research line is dedicated to Silicon photonic devices for telecommunication systems, while the other is dedicated to integrated systems for biophotonics, including optical trapping, optofluidics, acoustofluidics, single-cell analysis, and photomedicine. His current research interests are in the field of biodegradable and bioresorbable materials for photonic sensing applications.

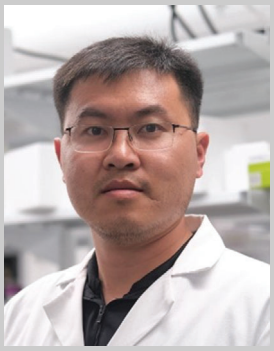

Jie Hui is currently a postdoctoral fellow at Massachusetts General Hospital and Harvard Medical School. He obtained his PhD in biomedical engineering from Purdue University and BS in applied physics from the University of Science and Technology of China. His research interests broadly lie in biophotonics, optical imaging, and phototherapy. His current research focuses on the development and clinical translation of drug-free antimicrobial phototherapy that was initiated by a serendipitously observed photobleaching phenomenon on S. aureus. His works were recognized by 2019 SPIE-Hillenkamp Postdoctoral Fellowship Award, 2024 QPC Lasers Young Investigator Best Paper Award, and 2024 SPIE Translational Research Award.

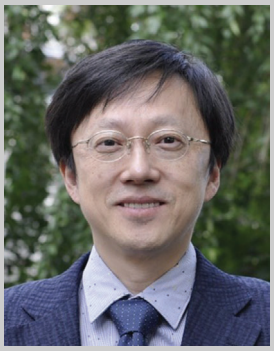

Seok-Hyun (Andy) Yun received his PhD degree in Physics from the Korea Advanced Institute of Science and Technology in 1997. He joined the Harvard Medical School and Massachusetts General Hospital as an Instructor in 2003 and rose to full Professor in 2017. He is the Director of the Harvard-MIT Summer Institute for Biomedical Optics. He published >250 papers and produced >100 patents. His research promoted the development of frequency-domain optical coherence tomography, Brillouin microscopy, bio-lasers, and laser particles. He has received the MGH Research Scholar Award, the NIH Director's Pioneer Award, and the NIH Director's Transformative Research Award.

Ali K. Yetisen is a Senior Lecturer and Associate Professor in the Department of Chemical Engineering at Imperial College London. He was previously a Tosteson fellow at Harvard University. He holds a PhD degree in Chemical Engineering and Biotechnology from the University of Cambridge. He aims to develop biochemical sensors, optical materials, and devices for application in medical diagnostics, therapeutics, and imaging. He has been awarded several international prizes including IChemE Nicklin Medal, a Fellowship of the Royal Society of Chemistry, a Fellowship of the Higher Education Academy, and a Fellowship of the Institute of Physics.